A METAL CATALYZED APPROACH FOR HETEROCYCLE COUPLING REACTIONS

A Thesis
Submitted to the Graduate Faculty
of the
North Dakota State University
of Agriculture and Applied Science

By

Michael Robert Chhoun

In Partial Fulfillment of the Requirements
for the Degree of
MASTER OF SCIENCE

Major Department:
Chemistry and Biochemistry

July 2021

Fargo, North Dakota

North Dakota State University
Graduate School

Title

A METAL CATALYZED APPROACH FOR HETEROCYCLE COUPLING REACTIONS

By

Michael Robert Chhoun

The Supervisory Committee certifies that this ***disquisition*** complies with North Dakota State University's regulations and meets the accepted standards for the degree of

MASTER OF SCIENCE

SUPERVISORY COMMITTEE:

Prof. Gregory R. Cook
Chair

Prof. Mukund P. Sibi

Prof. Alexey Leontyev

Prof. Mohi Quadir

Approved:

07/07/2021
Date

Prof. Gregory R. Cook
Department Chair

ABSTRACT

Heterocycles are cyclic compounds which contain atoms from at least two different elements. The work in this thesis describes methods we developed for the direct chemical transformation of indole heterocycles with various nitrogen heterocycles forming coupled heterocyclic compounds.

The first chapter of this thesis introduces background information of the heterocycles worked with on in our research. The chapter will discuss why the synthesis of these compounds are an interesting research topic.

The second chapter discusses the research of metal induced transformations of 4(3H)-quinazolinone. Specifically, the work that has been done in the literature to chemically transform these heterocycles.

The last chapter will discuss the investigation indole transformations that our group has developed using various reaction conditions. This will lead into discussion of the various methods that were developed by our group, possible mechanistic pathways, and future direction for this project.

ACKNOWLEDGEMENTS

I would like to thank Dr. Gregory R. Cook for welcoming me into his group. I have learned a lot over the years in the Cook group and I appreciate the opportunity to learn in your lab. I very much appreciated the open-door policy you had to discuss anything at anytime.

I would also like to thank my supervisory committee members Prof. Mukund P. Sibi, Prof. Alexey Leontyev, and Prof. Mohi Quadir. Thank you for the time you spent on my committee and for all the thoughtful input you have given me over the years. The advice you all have given me helped in research and in life.

I also want to thank my past group member Sandeepreddy Vemula for teaching me a lot about how to work in a research lab. Additionally, I want to thank the current Cook, Sibi, and Zhao group members for being available to help with my experiments or being available to talk about life. I wish the best for all of you whether it be research or life related.

Lastly, I would like to thank all the NDSU staff for assisting in the completion of my thesis. This includes Bonnie Hurner, Amy Kain, Cole Larsen, Brandon Gustafson, and Dr. Angel Ugrinov who were always there to lend a helping hand. Their expertise in their field is crucial for students completing their work.

TABLE OF CONTENTS

LIST OF TABLES

LIST OF FIGURES

LIST OF SCHEMES

LIST OF ABBREVIATIONS

AcOH	Acetic Acid
Ag	Silver
$AgSbF_6$	Silver hexafluoroantimonate
B	Broad
$B(Et)_3$	Triethylborane
$B(OH)_2$	Boronic acid
Bi	Bismuth
BQ	Benzoquinone
Br	Bromine
$C(Cp^3)$-H	Sp^3 hybridized carbon
C(1-7)	Carbon number (1-7)
Cbz	Benzyl chloroformate
C-C	Carbon carbon bond
C-H	Carbon hydrogen bond
CH_3CN	Acetonitrile
Cl	Chlorine
Co	Cobalt
C-O	Carbon Oxygen bond
CO_2	Carbon dioxide
CO_2Et	Ethyl ester group
Cp	Cyclopentadienyl
Cp*	Pentamethylcyclopentadiene
Cr	Chromium
$Cu(OMe)_2$	Copper(II)methoxide
d	Doublet
dd	Doublet of doublet
ddd	Doublet of doublet of doublet
C-X	Carbon halide/pseudohalide bond
DCE	Dichloroethane

DCM .....Dichloromethane

DMBQ.....2,6-Dimethylbenzoquinone

DMC .....Dimethylcarbonate

DMF.....Dimethylformamide

DMSO.....Dimethylsulfoxide

DMSO-D6.....Deuterated dimethylsulfoxide

EAS.....Electrophillic aromatic substitution

EDG .....Electron donating group

ESI.....Electron spray ionization

EWG .....Electron withdrawing group

FDA.....Food and Drug Administration

Fe.....Iron

Fe_2O_3.....Ferric Oxide

$FeCl_3$ .....Iron(III)Chloride

$FeCl_2$ .....Iron(II)Chloride

FG .....Functional group

GC.....Gas chromatography

H_2O .....Water

$HC(OMe)_3$.....Trimethyl orthoformate

HCl.....Hydrochloric acid

Hz.....Hertz

I .....Iodine

In .....Indium

J.....NMR coupling constant

KBr.....Potassium bromide

KCl.....Potassium chloride

KF .....Potassium flouride

$KMnO_4$.....Potassium permanganate

LA .....Lewis acid

LG .....Leaving group

Ln .....Ligand

M.....Metal

Mg-X.....Grignard reagent

MHz .....Megahertz

MS.....Mass Spectrometer

N1.....Nitrogen 1

$NaHCO_3$ .....Sodium Bicarbonate

N-heterocycle.....Nitrogen heterocycle

$NiCl_2$ .....Nickel(II)Chloride

NIS .....N-Iodosuccinimide

NMR .....Nuclear magnetic resonance

NO_3 .....Nitro group

NR.....No reaction

N-Ts .....Tosylated nitrogen

Nu.....Nucleophile

OAc.....Acetate

OMe .....Methoxy

OTf_3.....Triflate

Pd .....Palladium

$Pd(PPh_3)$.....Tetrakis(triphenylphosphine)palladium(0)

pH.....Power of hydrogen

Ph .....Phenyl

pKa.....Acid dissociation constant at logarithmic scale

ppm .....Parts per million

q.....Quartet

R.....Hydrocarbon group

Rh.....Rhodium

Ru.....Ruthenium

s .....Singlet

SbF_6.....Fluoroantimonic acid

SET .....Single electron transfer

$SnBu_3$ .....Organotin reagent

t .....Triplet

TBAI .....Tetrabutylammonium iodide

TBME .....Methyl tert-butyl ether

t-butyl.....Tert-butyl

TCA.....Trichloroacetic acid

TEMPO .....(2,2,6,6-Tetramethylpiperidin-1-yl)oxyl

TFA .....Triflouro acetic acid

THF .....Tetrahydrofuran

TLC .....Thin layer chromatography

$ZnCl_2$ .....Zinc(II)Chloride

LIST OF SYMBOLS

π .....Pi

e^-.....Electron

E^+ .....Electrophile

δ.....Delta

η^2 .....Eta 2

η^3 .....Eta 3

CHAPTER 1. RELEVENT N-HETEROCYCLIC STRUCTURES IN BIOLOGICALLY ACTIVE COMPOUNDS

1.1. Introduction

It is commonly known that nitrogen heterocycles (N-heterocycles) are common components in pharmaceutical compounds. Analyses of U.S. FDA approved drugs reveals that 59% of unique small-molecule drugs contain N-heterocycles[1]. Due to the relevance of the N-heterocycles in drug compounds, the development for the synthesis of large heterocyclic compounds is greatly desired.

1.2. Heterocycles: 4(3H)-Quinazolinone

Quinazoline and its derivatives are common alkaloid heterocycle found in medicinal compounds[2]. 4(3H)-Quinazolinone is an interesting derivative of quinazoline that has been found to be highly biologically active. 4(3H)-Quinazolinone constitutes an important class of fused heterocycles that accounts for more than 100 naturally occurring alkaloids. Many examples of quinazoline derivative drugs display biological effects that range from antibacterial, anticancer, and antifungal properties (Figure1). Therefore, development of innovative methodologies for the functionalization of this heterocycle is an appealing field of research.

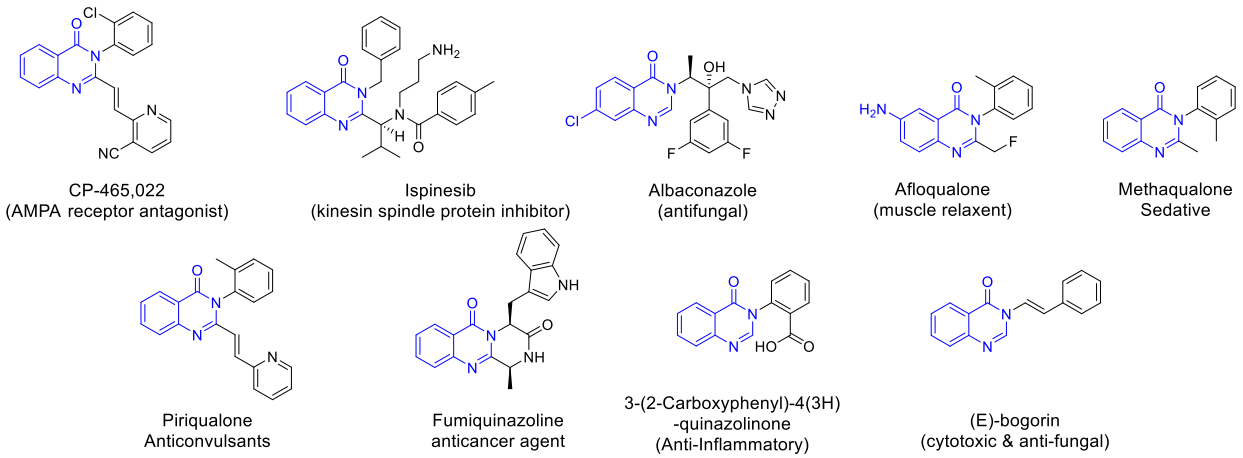

Figure 1.1: Examples of synthetic and natural quinazolinones identified with medicinal properties.

1.2.1. Heterocycles: 4(3H)-Quinazolinone Synthesis

Common methods for 4(3H)-Quinazolinone synthesis relies on cyclization type reactions such as the Niementowski reaction that involves the fusion of anthranilic acid with amides[3] (Scheme 1.1). Niementowski reaction is one of the most common methodologies for 4(3H)-Quinazolinone synthesis. The reaction proceeds through an amidobenzamide intermediate giving **1.01** as the product. Reaction yields can vary based on the substrate and the reaction temperatures making the reaction inconsistent when it comes to synthesizing a large array of 4(3H)-Quinazolinone derivatives.

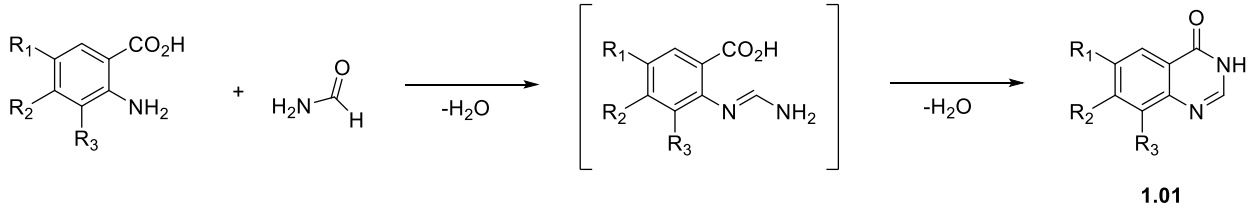

Scheme 1.1: Niementowski reaction example for synthesis of 4(3H)-Quinazolinone derivatives.

1.2.2. Antimicrobial Applications of 4(3H)-Quinazolinone Derivatives

As previously mentioned, 4(3H)-Quinazolinone and its derivatives are frequently found in pharmaceuticals. It has many applications in medicinal chemistry, but it particularly excels as an antibiotic[4]. This is promising due to the unmet needs for new types of antibiotics because of increasing drug resistance.

4(3H)-Quinazolinone has many positions available for tuning of antimicrobial activity[5]. The type of functionalization is dependent on the type of quinazolinone derivative being examined such as 2-thioquinazolin-4(3H)-one (**1.02**), 2-Styrylquinazolinone (**1.03**), or even multi heterocyclic derivatives (**1.04a-i**). It's been reported that functionalization of the 2-position with thiol functional groups results in high antimicrobial activity. 2-Thioquinazolin-4(3H)-one derivatives are highly dependent on the 3-positions being functionalized with benzyl groups to have high antimicrobial activity. This variation of quinazolinone had high antimicrobial activity when the 6-position was functionalized with EWG or EDG's (figure 2)[6].

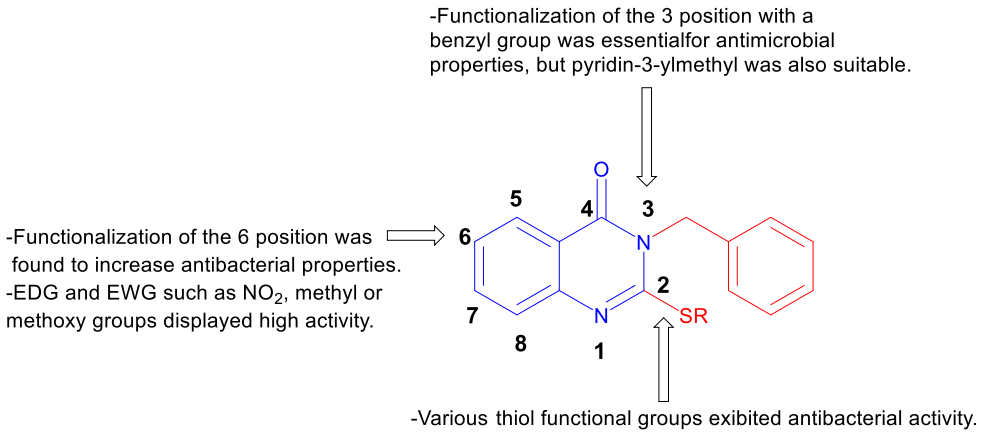

Figure 1.2: 4(3H)-Quinazolinone thiol derivatives (**1.02**) functionalization positions.

Substitution of the 2 positions with a styryl group to form styryl quinazolinone derivatives (**1.03**) displayed promising high antimicrobial activity[7]. Further substrate screening

revealed that the functionalization of the 3 positions with meta or ortho functionalized phenyl groups were preferred for antimicrobial activity.

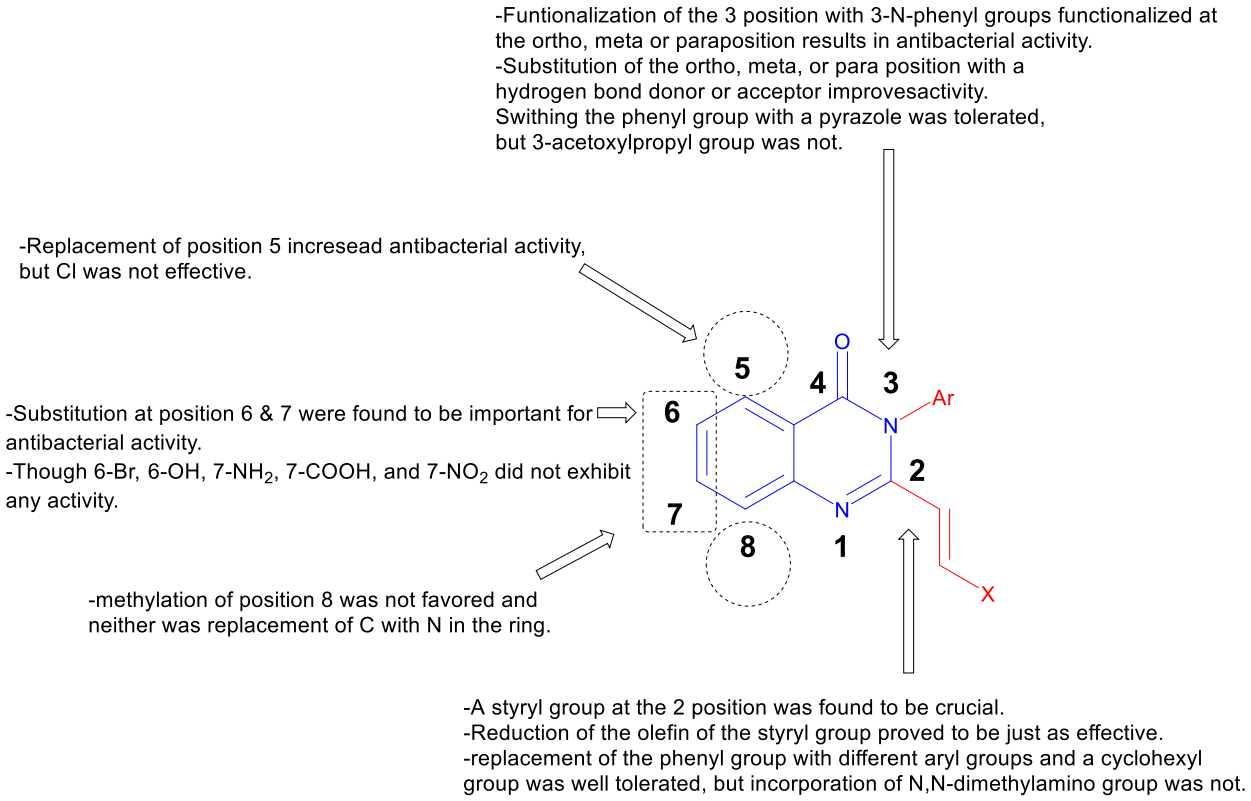

Figure 1.3: Styrylquinazolinone derivatives (**1.03**) that exhibit promising antimicrobial properties.

Sulfonamide, triazoepino quinazolinones and triazocino quinazolinone derivatives prepared from amino acids to form fused heterocyclic systems showed modest to high activity (Figure 4, structures **1.04a-c**)[8]. Additionally, functionalization of the 3-position with various heterocycles such as thioureas, thiazolines and thiazolidinones proved very effective (Figure 1.4, **1.04g-i**).

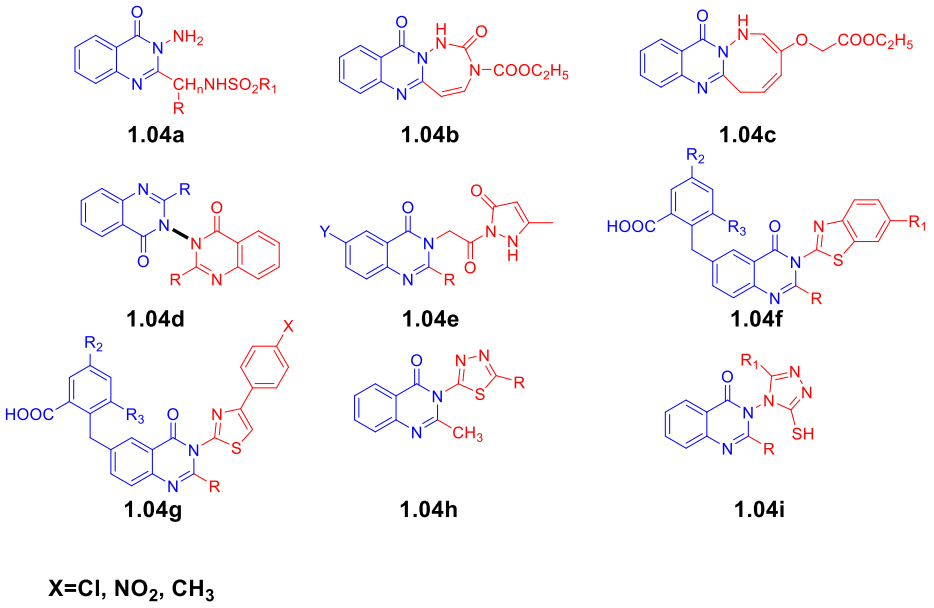

Figure 1.4: Multi-heterocyclic 4(3H)-Quinazolinone that display high antimicrobial activity (**1.04a-i**).

1.3. Heterocycles: Indole

Indole is an example of a naturally occurring structure that is present in many natural products [9]. It is a privileged structure that has been integral in the pharmaceutical, fragrance, agrochemical, pigment, and material science field. However, the most intensely researched application tends to be pharmaceutical related. Indoles and its derivatives are often synthesized through cyclization methodologies such as Fischer indole synthesis (Scheme 1.2)[10].

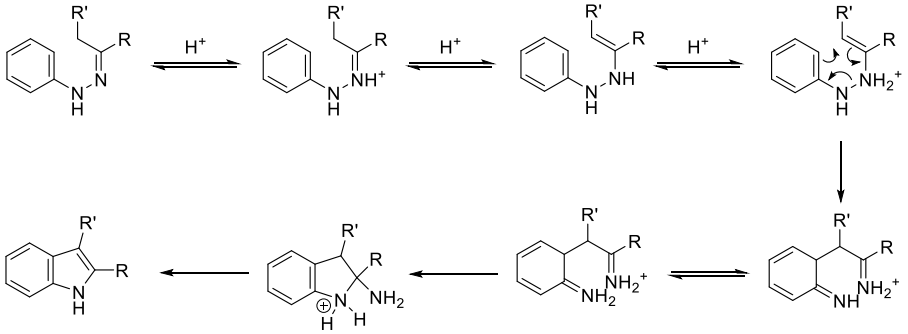

Scheme 1.2: Fischer indole synthesis mechanism.

Though cyclization reactions are an effective way to form various indoles; much interest lately has been focused on functionalizing of the preformed indole. Cyclization reactions often require specific substrates to synthesize more complex indole structures. Additionally, cyclization reactions do not allow for late-stage functionalization whereas direct coupling between two different heterocycles would.

1.3.1. Indole Functionalization

Indole is an electron-rich heteroaromatic compound that has high susceptibility to electrophilic aromatic substitution reactions (EAS). That is something that must be considered when working with indole compounds to avoid unwanted product. The C3 position of indole is typically the most prone to EAS reactions (Figure 1.5).

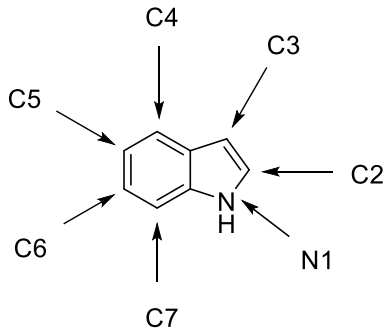

Figure 1.5: Indole structure, and reactive positions.

Occupation of the C3 position tends to result in increased reactivity of the C2 position which is attributed to the electronics of the indole ring. There are significantly more reports of C3 functionalization compared to C2 position. Positions C4-C7 are rarer than positions C2 and C3 due to the high reactivity of the C2 and C3 position. Indole has the highest reactivity in the C3 position to electrophiles. Many have reported umpolung strategies to functionalize the C2 position (figure 6)[11].

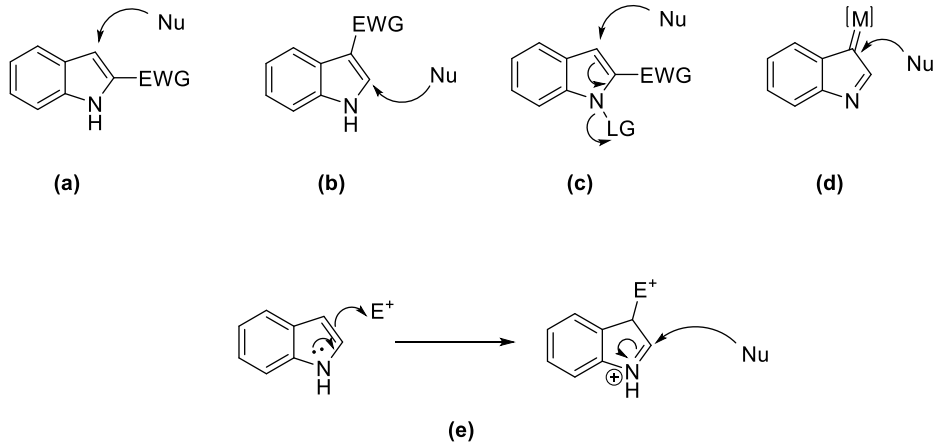

Figure 1.6: Umpolung methods for C3 & C2 functionalization.

The C3 position is the most nucleophilic position on the indole ring, but installation of an EWG at the C2 position inverts the reactivity resulting in nucleophilic attacks becoming possible at the C3 position (Figure 1.6a). The reverse has been displayed by installing an EWG at the C3 position to get nucleophilic attack at the C2 position (Figure 1.6b). Installation of leaving groups (LG) at the N1 position in the presence of a EWG at the C2 position allows for the functionalization of the C3 position with a nucleophile (Figure 1.6c). Metal carbene intermediates have been used to increase reactivity at the C3 position to allow selective C3 functionalization with a nucleophile (Figure 1.6d). An alternative umpolung method is to use an electrophile/Lewis acid (LA) to react with the C3 position to form an electrophilic iminium intermediate that reacts with a nucleophile at the C2 position (Figure 1.6e). Re-aromatization is dependent on the electrophiles ability to act as a LG.

1.3.2. Significance of Indole Multi-heterocyclic Systems

4(3H)-Quinazolinone and indole compounds have been reported to have high biological activity in structures such as rutecarpine **(1.06**) and dihydrorutecapin (**1.05**)[12]. Seidel and co-workers reported a methodology of synthesizing deoxyvasicinone (**1.07**) and rutaecarpine (**1.06**) by the $KMnO_4$ promoted oxidation of aminals[13,14]. Examples of muti-heterocyclic systems

incorporating quinazolinone and indole ring were shown through Bergmans procedure to form dihydrorutaempine (**1.06**) which has shown a variety of intriguing biological properties such as anti-thrombotic, anticancer, anti-inflammatory and analgesic, anti-obesity and thermoregulatory, vasorelaxing activity[15].

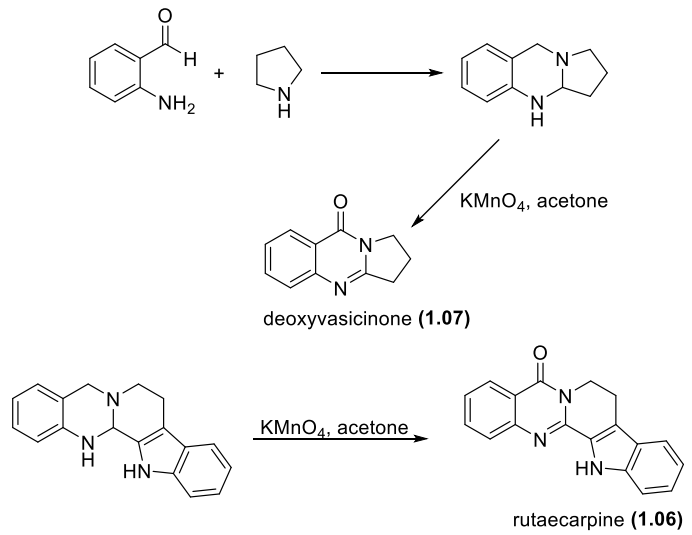

Scheme 1.3: Established procedure for synthesis of deoxyvasicinone (**1.07**) and rutecarpine (**1.06**).

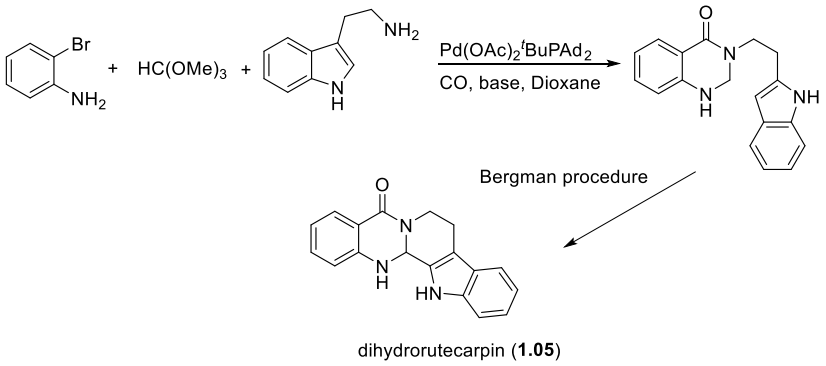

Scheme 1.4: Established procedure for synthesis of dihydrorutecarpin (**1.05**).

1.4. References

(1) Vitaku, E.; Smith, D. T.; Njardarson, J. T. Analysis of the Structural Diversity, Substitution Patterns, and Frequency of Nitrogen Heterocycles among U.S. FDA Approved Pharmaceuticals. *J. Med. Chem.* **2014**, *57* (24), 10257–10274. https://doi.org/10.1021/jm501100b.

(2) Auti, P. S.; George, G.; Paul, A. T. Recent Advances in the Pharmacological Diversification of Quinazoline/Quinazolinone Hybrids. *RSC Adv.* **2020**, *10* (68), 41353–41392. https://doi.org/10.1039/d0ra06642g.

(3) Niementowski, S. Synthesen Der Chinolinderivate. *Chemische Berichte*. **1894**, *27* (2), 1394–1403. https://doi.org/10.1002/cber.18940270242.

(4) Gatadi, S.; Lakshmi, T. V.; Nanduri, S. 4(3H)-Quinazolinone Derivatives: Promising Antibacterial Drug Leads. *Eur. J. Med. Chem.* **2019**, *170*, 157-172. https://doi.org/10.1016/j.ejmech.2019.03.018.

(5) Ugale, V. G.; Bari, S. B. Structural Exploration of Quinazolin-4(3H)-Ones as Anticonvulsants: Rational Design, Synthesis, Pharmacological Evaluation, and Molecular Docking Studies. *Arch. Pharm. (Weinheim).* **2016**, *349* (11), 864–880. https://doi.org/10.1002/ardp.201600218.

(6) Alagarsamy, V.; Murugesan, S.; Dhanabal, K.; Murugan, M.; De Clercq, E. Anti-HIV, Antibacterial and Antifungal Activities of Some Novel 2-Methyl-3-(Substituted Methylamino)-(3H)-Quinazolin-4-Ones. *Indian J. Pharm. Sci.* **2007**, *69* (2), 304–307. https://doi.org/10.4103/0250-474X.33167.

(7) Bouley, R.; Kumarasiri, M.; Peng, Z.; Otero, L. H.; Song, W.; Suckow, M. A.; Schroeder, V. A.; Wolter, W. R.; Lastochkin, E.; Antunes, N. T.; Pi, H.; Vakulenko, S.; Hermoso, J. A.; Chang, M.; Mobashery, S. Discovery of Antibiotic (E)-3-(3-Carboxyphenyl)-2-(4-Cyanostyryl)Quinazolin-4(3 H)-One. *J. Am. Chem. Soc.* **2015**, *137* (5), 1738–1741. https://doi.org/10.1021/jacs.5b00056.

(8) Haseena, B.; Prasad, K.V.S.R.G.; Bharathi, K. Biological Importance of Quinazolin-4-One Scaffold and Its Derivatives-a Brief Update. *Int. J. Pharm. Pharm. Sci.* **2015**, *7* (6), 1–7.

(9) Kaushik, N. K.; Kaushik, N.; Attri, P.; Kumar, N.; Kim, C. H.; Verma, A. K.; Choi, E. H. Biomedical Importance of Indoles. *Molecules.* **2013**, *18* (6), 6620–6662. https://doi.org/10.3390/molecules18066620.

(10) Fischer, E.; Jourdan, F. Ueber Die Hydrazine Der Brenztraubensäure. *Berichte der Dtsch. Chem. Gesellschaft.* **1883**, *16* (2), 2241–2245. https://doi.org/10.1002/cber.188301602141.

(11) Deka, B.; Deb, M. L.; Baruah, P. K. Recent Advances on the C2-Functionalization of Indole via Umpolung; *Top Curr Chem*, **2020**; 378(22), 1-32. https://doi.org/10.1007/s41061-020-0287-7.

(12) Son, J. K.; Chang, H. W.; Jahng, Y. Progress in Studies on Rutaecarpine. II.-Synthesis and Structure-Biological Activity Relationships. *Molecules.* **2015**, *20* (6), 10800–10821. https://doi.org/10.3390/molecules200610800.

(13) Zhang, C.; De, C. K.; Mal, R.; Seidel, D. α-Amination of Nitrogen Heterocycles: Ring-Fused Aminals J. Am. Chem. Soc. 2008, 130, 416– 417. https://doi.org/10.1021/ja077473r.

(14) Dieckmann, A.; Richers, M. T.; Platonova, A. Y.; Zhang, C.; Seidel, D.; Houk, K. N. Metal-Free α-Amination of Secondary Amines: Computational and Experimental Evidence for Azaquinone Methide and Azomethine Ylide Intermediates. *J. Org. Chem.* **2013**, 78, 4132– 4144. https://doi.org/10.1021/jo400483h

(15) L. He, H. Li, H. Neumann, M. Beller.; X.F. Wu. Highly efficient four-component synthesis of 4(3H)-quinazolinones: palladium-catalyzed carbonylative coupling reactions. *Angew.Chem. Int. Ed.*, **2014**, 53, 1420–1424. https://doi.org/10.1002/anie.201308756.

CHAPTER 2. TRANSITION METAL MEDIATED N-HETEROCYLE FUNCTIONALIZATION

2.1. Introduction

Traditional organic synthesis involves transformation of a pre-existing functional groups into a new desired functional group. Though effective, traditional organic reactions have limitations. Though many regio-and/or chemoselective issues can achieved through a variety of organic reagents, multiple reaction steps are often required. Transition metal catalyzed cross-coupling reactions have since become an appealing method to overcome limitations present in traditional organic synthesis (Figure 2.1)[1]. Transition metal catalyzed cross-coupling reactions are a powerful tool for synthesis of natural products, pharmaceuticals, and polymers. They allow for facile synthesis of large compounds under simplistic and mild reaction conditions. The advent of C-H activation has increased the utility of transition metal catalyzed reactions even more so providing access many more synthesizable compounds[2]. The variation of cross-coupling reactions is vast and will not be discussed in full detail, but the methodology for applying transition metal catalyzed cross-coupling reactions to N-heterocycle functionalization will be discussed as it is the focus of this work.

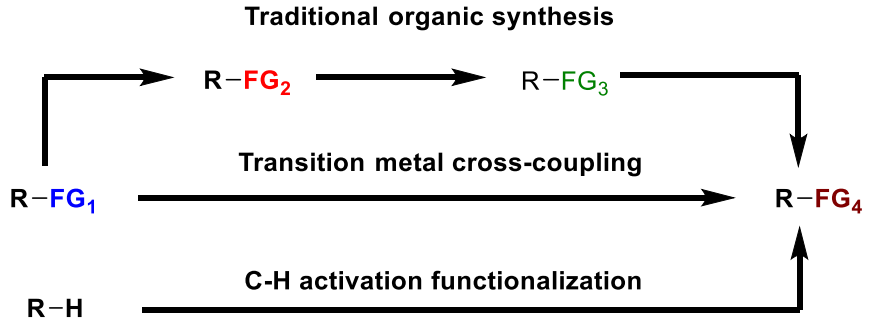

Figure 2.1: Traditional organic synthesis pathway vs transition metal catalysis pathway.

2.2. Transition Metal Catalyzed Functionalization

In 1972, cross-coupling chemistry saw a major development when Tamao-Kumada-Corriu coupling was reported which allowed for the coupling of Grignard reagents with organic halides to form C-C bonds[3,4]. In addition to Tamao-Kumada-Corriu coupling, other reactions such as Suzuki-Miyaura coupling, Stille coupling, Negishi coupling, and Sonogashira coupling were reported throughout the years (Figure 2.1)[5,6,7]. The use of transition metals allowed synthetic chemist to conduct synthesis of large complex molecules rapidly, and efficiently. Palladium catalyzed cross-coupling reactions are one of the more notable reactions due to its ability to easily generate C-C and C-X bonds.

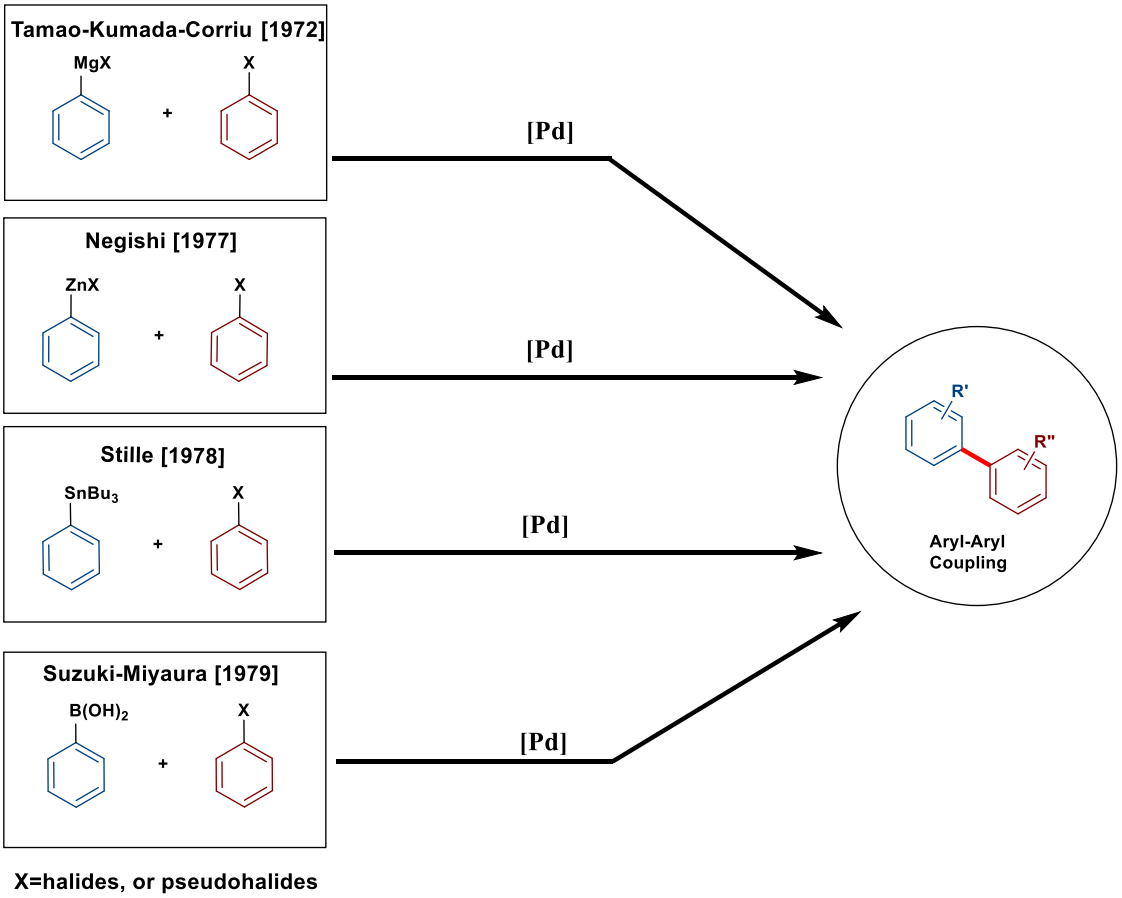

Figure 2.2: Summary of highly impactful cross-coupling reactions.

Cross-coupling reactions typically utilize pre-oxidized coupling partners that undergo oxidative addition in the first step of the catalytic cycle. In the case of palladium catalyzed cross-coupling, the Pd forms Pd(II) after oxidative addition to form an organopalladium intermediate (Scheme 2.1). Then it is followed up by transmetallation and reductive elimination. Oxidative addition is involved in many transition metal catalyzed cross-coupling reactions. It is also the first step in Tsuji-Trost allylation which is one of the focal points of the work discussed[7,8].

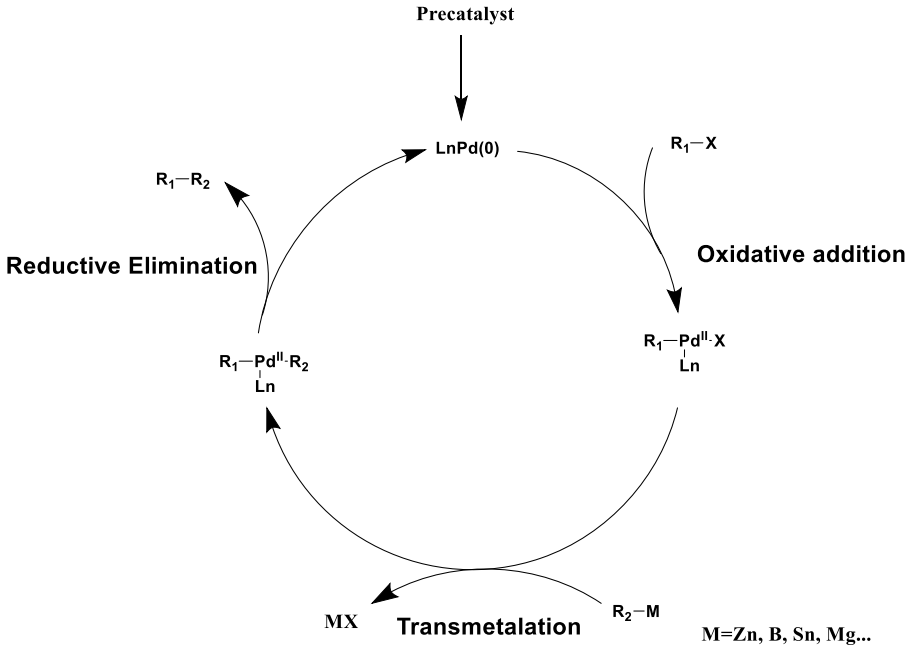

Scheme 2.1: Mechanism of Suzuki-Miyaura cross-coupling.

2.2.1. Tsuji-Trost Allylation

Tsuji-Trost allylation utilizes oxidized substrates to form C-C and C-X bonds utilizing allyl substrates (Scheme 2.2). The palladium catalyzed cross-coupling of allyl electrophiles with nucleophiles has become a power tool in the literature for achieving selective allylation of nucleophiles[9].

Stoichiometric Tsuji-Trost allylation

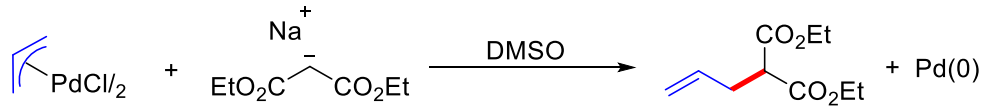

Scheme 2.2: First reported Tsuji-Trost allylation reaction.

Major strides in Tsuji-Trost allylation came when the reaction was developed into a catalytic reaction by Trost and co-workers. The use of oxidized allyl substrates containing leaving groups also revolutionized the utility of the reaction. Stoichiometric palladium is not ideal due to its high toxicity and high cost. Trost and co-workers utilized phosphine ligands to catalytically generate π-allyl-palladium (**2.01**) which catalyzes the allylation reaction (Scheme 2.03).

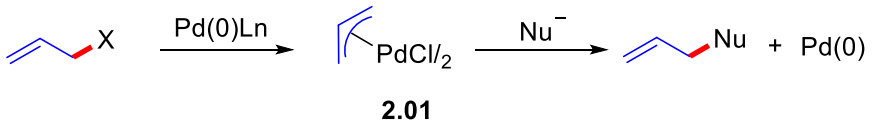

2.01

Scheme 2.3: First reported catalytic Tsuji-Trost allylation.

2.2.2. Mechanism of Tsuji-Trost Allylation

The generally accepted mechanism of Tsuji-Trost allylation is depicted below (Scheme 2.4)[10]. The mechanism begins with Pd(0) coordinating to the allylic olefin forming an η^2-complex (**2.02**), which is followed up by oxidative addition of the allyl forming a 16 e^- (η^3-allyl)Pd(II) complex (**2.03**). The nucleophile then attacks at terminal position which results in the alyllated product (**2.04**) and a Pd(0) species coordinating on to the newly formed allyl species which is easily released and continues the catalytic cycle.

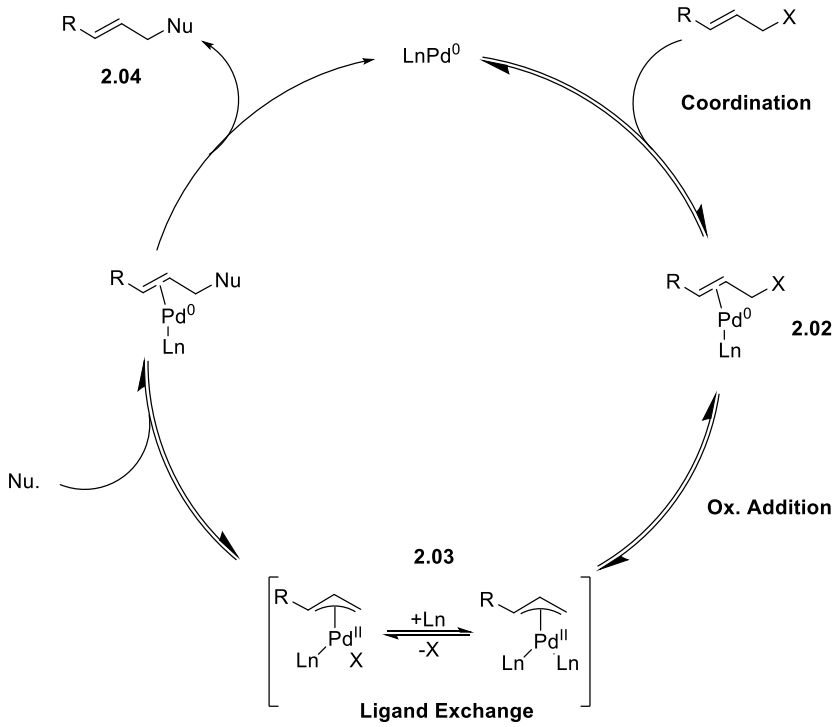

Scheme 2.4: Generally accepted Tsuji-Trost allylation reaction mechanism.

2.2.3. Regioselective Tsuji-Trost Allylation

Regio- and chemo selectivity is a challenging issue to overcome when it comes to natural product synthesis. This is an issue when it comes to N-heterocycles with multiple nucleophilic centers. Tautomerizable heteroarenes, such as 4(3H)-Quinazolinone, or 2-Hydroxypyridine are examples of N-heterocycles with multiple nucleophilic centers. Depending on reaction conditions; it has the potential to result in allylation at three separate reaction sites which would allow for a mixture of products (**2.05, 2.06, 2.07**).

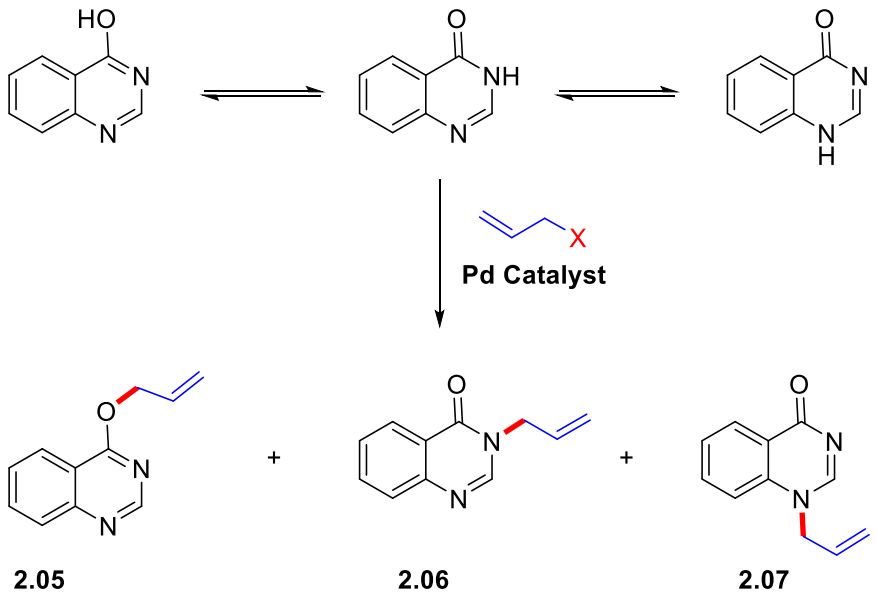

Scheme 2.5: Pathways of allylation of 4(3H)-Quinazolinone.

Our group has focused our efforts on development of efficient catalytic for the functionalization of tautomerizable heterocycles. The work begun with allylation of 4-3(H)-Quinazolinone under various conditions. The appeal of allylation reactions stem from their ability to be transformed into a variety of useful functional groups. Many allylation type reactions were successfully developed for the 4-3(H)-Quinazolinone motif. The work led to various other types of promising reactions that could lead to the discovery of useful 4-3(H)-Quinazolinone derivatives.

2.3. Allylation of 4(3H)-Quinazolinone

The leaving group ability of allylic compounds have since been extensively explored since Tsuji first reported the Tsuji-Trost allylation[11]. Typically, halogens have performed as the best allyl substrate due good leaving group ability of halides. However, allyl alcohols do not have that luxury due to the strong C-O bonds which renders it an unfavorable leaving group. Utilization of allyl alcohols is beneficial due to their wide availability, and low toxicity. Additionally, the generation of water as a byproduct when using allyl alcohols reduces

generation of halogenated waste. Overcoming the strong C-O bond has been overcome using additives such as Lewis and Bronsted acids or by in-situ generation of carbonate via CO_2 as a reversible activator[12,13,14,15]. The downfall of these strategies includes stoichiometric amounts of additives needed, poor reaction scope, or the use of specialized conditions. Allyl alcohols have been shown in the literature to be suitable substrates for Tsuji-Trost allylation in the literature, but suffer from high reaction temps, and lack of selectivity[16]. This section discusses the work our group has done using allyl alcohols for the regioselective allylation of 4(3H)-Quinazolinone which includes methodology development and mechanistic discussions[17].

Initial screening revealed that allyl alcohol in the presence of $Pd(PPh_3)_4$ was able to successfully allylate 4(3H)-Quinazolinone regioselectively (**2.08**) with no other allylated by-products detected. Upon discovering that the reaction could be done efficiently the solvent conditions were then explored. Dimethyl carbonate (DMC) showed that it was the optimal solvent for the reaction. DMC is an appealing solvent due to its low toxicity, renewability, and biodegradability therefore was chosen as the solvent media. After an overall extensive screening process, our group reported the reaction conditions below which show that 5 mol% $Pd(PPh_3)_4$, 1.2 equiv. allyl alcohol, in DMC at 100 °C for 12 h was the optimal reaction conditions (Scheme 2.6).

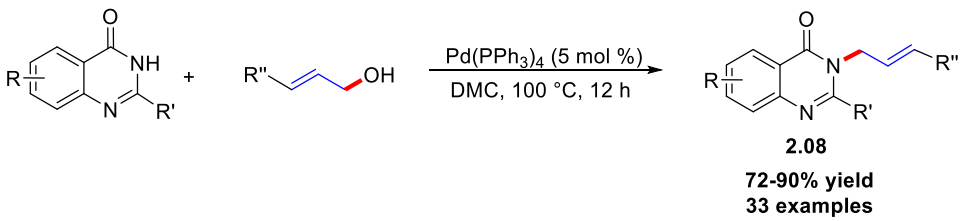

Scheme 2.6: Established protocol of allylation of 4(3H)-Quinazolinone to form compound **2.08**.

2.3.1. Palladium Catalyzed Allylic C-H Activation

Using C-H bond activation methodology allows the synthesis of complex molecules that play roles in total synthesis, materials, and medicinal compounds. C-H bonds are present in most organic molecules, however they lack reactivity[18,19]. The poor reactivity of C(Sp^3)–H bonds can be attributed to their bond energies (typically 90–100 kcal/mol), low acidity (estimated pKa = 45 to 60), and unreactive molecular orbital profile that make it tough to selectively cleave[20]. Some researchers have reported methods of overcoming this by taking advantages of directing groups[21]. Allylic C-H bonds have decreased bond dissociation energy relative to aliphatic C-H bonds, and the presence of the olefin can act as a directing group for selective C-H bond cleavage[22]. Though this methodology does have its benefits, many outlined conditions contain many additives to activate the allylic C-H bond due to its low reactivity. The complex mixtures usually required may result in the formation of unwanted byproducts or poor yields. Using a good leaving group allows for fast allyl ionization followed by a nucleophilic attack, which is not the case for allylic C-H activation. The challenge of allylic C-H activation comes from the convoluted mechanism which requires three separate steps for C-H cleavage, nucleophilic attack, and Pd(II) oxidation to Pd(0).

White and co-workers developed a methodology for allylic C-H activation utilizing a Pd(II)/bis-sulfoxide system which was originally reported as allylic acetoxylation (Scheme 2.07)[23], and esterification[24] but expanded to C-C bond formation[25]. White and co-workers reported the first intramolecular allylic C-H amination to generate *anti*-oxazlidinone products (**2.10**)[26]. Allylic C-H amination requires a weak Lewis basic nucleophile to prevent interference with the C-H cleavage step, and is also acidic enough to be deprotonated by the Pd(II) counter ion. Intramolecular amination also faces the issue of regio-, and chemoselectivity. White and co-

workers were able to tether N-Tosyl carbamate (**2.09**) via intramolecular C-H activation. Mechanistic studies revealed the generation of π-allyl palladium intermediate. The palladium catalyst counter ion acts as an exogeneous base deprotonating the tethered nucleophile which allows the tethered nucleophile to attack the π-allyl intermediate forming a five membered ring followed by quinone regenerating the catalyst acting as an oxidant (Scheme 2.7).

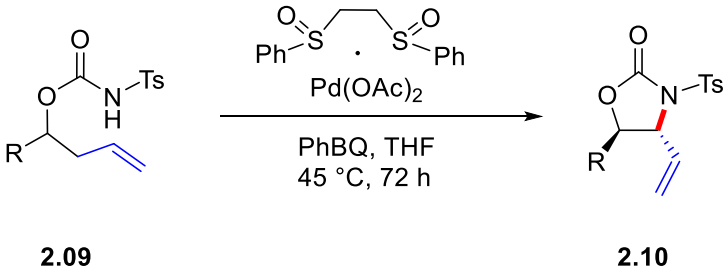

2.09 **2.10**

Scheme 2.7: White and co-workers first intramolecular allylic C-H amination reaction to generate *anti*-oxazolidinone products (**2.10**).

Intermolecular allylic C-H amination is even more challenging due to the possibility of olefin isomerization and meeting the electronic demands required to induce all the steps required for allylic C-H activation. Early studies reported for allylic C-H activation heavily relied on super stoichiometric amounts of oxidants. White and co-workers utilized the Lewis acid Cr(III)(salen)Cl to assist in inducing the nucleophilic attack on the palladium π -allyl species (Scheme 2.8). Stoichiometric amount of Cr(III)(Salen)Cl was found to successfully promote intermolecular C-H amination generating structure **2.11** with high regio- and chemo-selectivity[27]. It was suggested that the Lewis acid increased the electrophilic nature of the BQ bound palladium π -allyl complex (**2.12**), which assisted in the nucleophilic attack (Scheme 2.9).

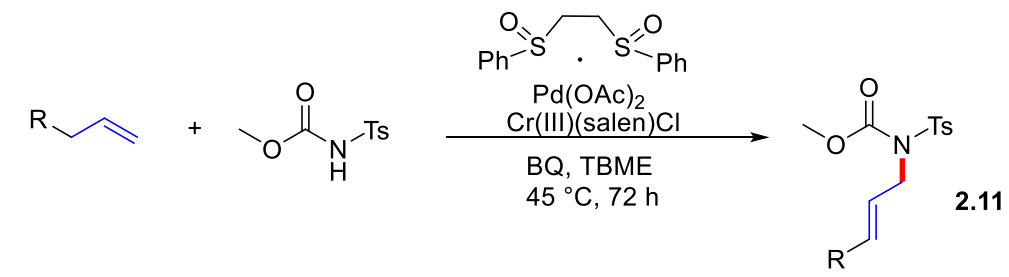

Scheme 2.8: Intermolecular allylation using Cr(III)(salen)Cl as a Lewis acid to form product **2.11**.

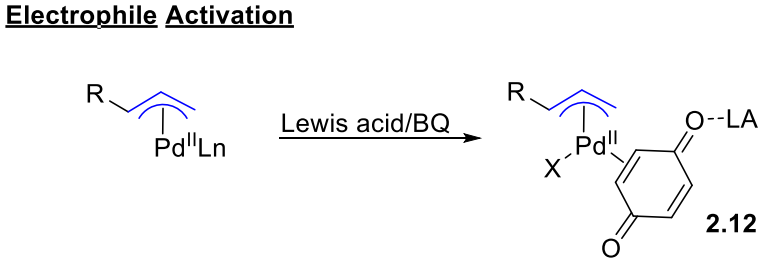

Scheme 2.9: Proposed Lewis acid bound BQ palladium π-allyl complex (**2.12**).

2.3.2. Tsuji-Trost Allylation of 4(3H)-Quinazolinone via Allylic C-H Activation

Success of the Tsuji-Trost allylation via allyl alcohols motivated our group to expand into allylic C-H activation on tautomerizable N-heterocycles such as 4(3H)-Quinazolinone[28]. The initial investigation was started using White and co-workers established conditions for allylic C-H allylation of 4(3H)-Quinazolinone with allyl benzene. Initially, the experiment begun with the use of Whites catalyst, BQ, TBME, and Lewis acids. Under these conditions, no product was observed with any of the Lewis acids screened. Solvent and temperature screening gave no product, which reveals that White's conditions aren't suitable for this reaction. Screening revealed that $PdCl_2$ with DMBQ as the oxidant in DMSO was effective for the reaction, resulting in allylated 4(3H)-Quinazolinone (**2.13**). It is theorized that DMSO was necessary due to its coordination ability. The reaction was deemed optimal at 100 °C and was highly dependent on that elevated temperature (Scheme 2.10).

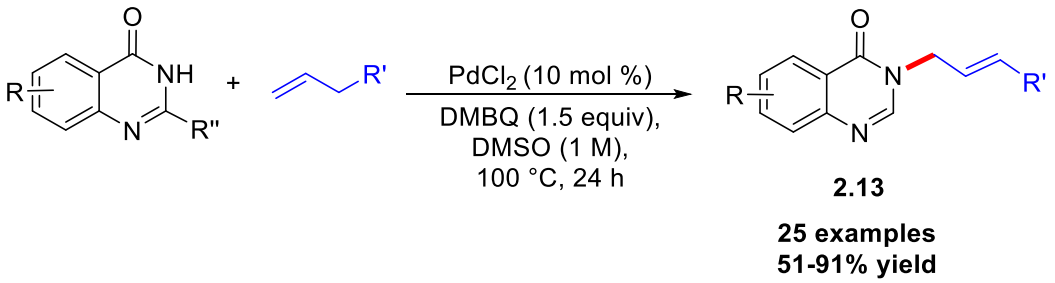

Scheme 2.10: Optimal conditions for our allylic C-H activation reaction yielding structure **2.13**.

2.3.3. 4(3H)-Quinazolinone via Allylic C-H Activation Mechanism

The speculated mechanism involves the formation of π-allyl palladium complex (**2.14**) as the key intermediate, which is formed by the electrophilic allylic C-H bond cleavage by sulfoxide-assisted palladium catalyst. This then allows the N-heterocycle to attack the π-allyl palladium species (**2.15**), followed by the regeneration of Pd(II) by DMBQ via oxidation (**2.16**). To validate the mechanism, stoichiometric amounts of the palladium was used in the reaction that did not include the nucleophile and monitored by H-NMR. Dimeric π-allyl palladium chloride complex was observed, which supports the π-allyl palladium pathway. No π-allyl palladium was observed in the absence of DMSO (using other solvents) suggesting that the DMSO plays a role in the π-allyl palladium intermediate formation (Scheme 2.11).

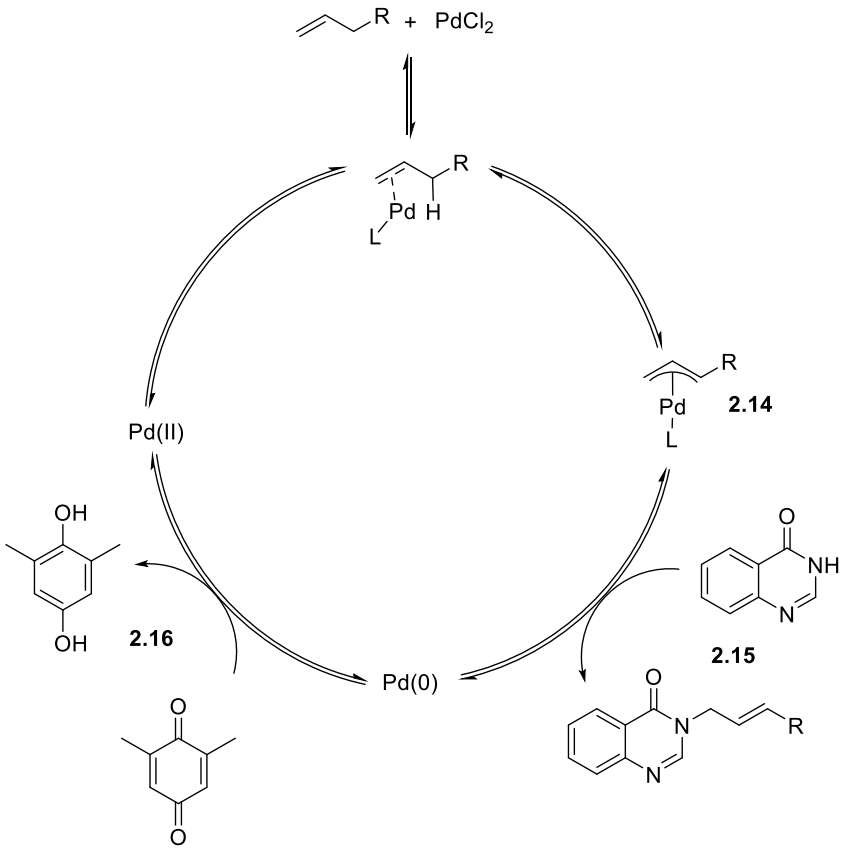

Scheme 2.11: Proposed mechanism of our reported allylic C-H activation reaction.

2.4. References

(1) Biffis, A.; Centomo, P.; Del Zotto, A.; Zecca, M. Pd Metal Catalysts for Cross-Couplings and Related Reactions in the 21st Century: A Critical Review. *Chem. Rev.* **2018**, *118* (4), 2249–2295. https://doi.org/10.1021/acs.chemrev.7b00443.

(2) Crabtree, R. H.; Lei, A. Introduction: C-H Activation. *Chem. Rev.* **2017**, *117* (13), 8481–8482. https://doi.org/10.1021/acs.chemrev.7b00307.

(3) J.P. Corriu, J. P. M. Activation of Grignard Reagents by Transition-Metal Complexes. A New and Simple Synthesis of Trans-Stilbenes and Polyphenyls. *J. Chem. Soc., Chem. Commun.* **1972**, *3* (144), 7062. https://doi.org/10.1039/C3972000144A.

(4) Tamao, K.; Sumitani, K.; Kumada, M. Selective Carbon-Carbon Bond Formation by Cross-Coupling of Grignard Reagents with Organic Halides. Catalysis by Nickel-Phosphine Complexes. *J. Am. Chem. Soc.* **1972**, *94* (12), 4374–4376. https://doi.org/10.1021/ja00767a075.

(5) Miyaura, N.; Yamada, K.; Suzuki, A. A New Stereospecific Cross-Coupling by the Palladium-Catalyzed Reaction of 1-Alkenylboranes with 1-Alkenyl Halides. *Tetrahedron Lett.* **1979**, *20* (36), 3437–3440.

(6) Sonogashira, K. Development of Pd-Cu Catalyzed Cross-Coupling of Terminal Acetylenes with Sp^2-Carbon Halides. *J. Organomet. Chem.* **2002**, *653* (1–2), 46–49. https://doi.org/10.1016/S0022-328X(02)01158-0.

(7) Tsuji, J. Organic Syntheses by Means of Noble Metal Compounds. *Nippon kagaku zassi* **1967**, *88* (7), 687–706. https://doi.org/10.1246/nikkashi1948.88.7_687.

(8) Trost, B. M., Fullerton, T. J. New Synthetic Reactions. Allylic Alkylation. *J. Am. Chem. Soc.* **1973**, *95* (1), 292–294. https://doi.org/10.1021/ja00782a080.

(9) Smidt, J.; Haftner, W.; Jira, R.; Sedlmeier, J.; Sieber, R.; Rüttinger, R.; Kojer, H. Katalytische Umsetzungen von Olefinen an an Platinmetall-Verbindungen. *Angew. Chemie* **1959**, *71* (5), 176–182. https://doi.org/10.1002/ange.19590710503.

(10) Trost, B. M.; Sieber, J. D. The Palladium Catalyzed Asymmetric Addition of Oxindoles and Allenes : An Atom- Economical Versatile Method for the Construction of Chiral Indole Alkaloids Supplementary Material Part A : Experimental Section. *J. Am. Chem. Soc.* **2011**, *133* (Scheme 2), 20611–20622. https://doi.org/10.1021/ja209244m.

(11) Trost B.M. Metal Catalyzed Allylic Alkylation: Its Development in the Trost Laboratories. *Physiol. Behav.* **2016**, *176* (1), 100–106. https://doi.org/10.1016/j.tet.2015.06.044.Metal.

(12) Kokatla, H. P.; Lakshman, M. K. One-Pot Etherification of Purine Nucleosides and Pyrimidines. *Org. Lett.* **2010**, *12* (20), 4478–4481. https://doi.org/10.1021/ol101655h.

(13) Wang, Y.; Zhang, M.; Cao, S.; Lin, H.; Gao, M.; Li, Z. Synthesis of 1-Substituted 4(1H)-Quinazolinones under Solvent-Free Conditions. *Synth. Commun.* **2012**, *42* (18), 2715–2727. https://doi.org/10.1080/00397911.2011.566407.

(14) Paquin, F.; Rivnay, J.; Salleo, A.; Stingelin, N.; Silva, C. Multi-Phase Semicrystalline Microstructures Drive Exciton Dissociation in Neat Plastic Semiconductors. *J. Mater. Chem. C* **2015**, *3*, 10715–10722. https://doi.org/10.1039/b000000x.

(15) Golfier, M; Milcent, R. Reaction of Acylhydrazines with Phenyltrichloromethane; A Simple Synthesis of N-Acyl-Phenylmethanehydrazonates and 1,3,4-Oxadiazoles. *Synthesis (Stuttg).* **1979**, No. 12, 946–948. https://doi.org/10.1055/s-1979-28882

(16) Zhang, J.; Liao, J.; Wei, Y.-F.; Cheng, G.; Luo, R. Recent Advance of Allylic Alcohol Reagents in Organic Synthesis. *Mini. Rev. Org. Chem.* **2018**, *15* (6), 476–487. https://doi.org/10.2174/1570193x15666180220125122.

(17) Kumar, D.; Vemula, S. R.; Cook, G. R. Highly Chemo- and Regioselective Allylic Substitution with Tautomerizable Heteroarenes. *Green Chem.* **2015**, *17* (8), 4300–4306. https://doi.org/10.1039/c5gc01028d.

(18) Ryabov, A. D. Mechanisms of Intramolecular Activation of C-H Bonds in Transition-Metal Complexes. *Chem. Rev.* **1990**, *90* (2), 403–424. https://doi.org/10.1021/cr00100a004.

(19) Forsman, Å.; Grimvall, A. Reduced Models for Efficient Simulation of Spatially Integrated Outputs of One-Dimensional Substance Transport Models. *Environ. Model. Softw.* **2003**, *18* (4), 319–327. https://doi.org/10.1016/S1364-8152(03)00005-7.

(20) Balcells, D.; Clot, E.; Eisenstein, O. C-H Bond Activation in Transition Metal Species from a Computational Perspective. *Chem. Rev.* **2010**, *110* (2), 749–823. https://doi.org/10.1021/cr900315k.

(21) Hashiguchi, B. G.; Bischof, S. M.; Konnick, M. M.; Periana, R. O. Y. A. Designing Catalysts for Functionalization of Unactivated C-H Bonds Based on the C-H Activation Reaction. *IUPAC Compend. Chem. Terminol.* **2008**, *45* (6), 885–898. https://doi.org/10.1351/goldbook.a00103.

(22) Labinger, J. A.; Bercaw, J. E. Understanding and Exploiting C-H Bond Activation. *Nature* **2002**, *417* (6888), 507–514. https://doi.org/10.1038/417507a.

(23) Chen, M. S.; Prabagaran, N.; Labenz, N. A.; White, M. C. Serial Ligand Catalysis: A Highly Selective Allylic C-H Oxidation. *J. Am. Chem. Soc.* **2005**, *127* (19), 6970–6971. https://doi.org/10.1021/ja0500198.

(24) Delcamp, J. H.; White, M. C. Sequential Hydrocarbon Functionalization: Allylic C-H Oxidation/Vinylic C-H Arylation. *J. Am. Chem. Soc.* **2006**, *128* (47), 15076–15077. https://doi.org/10.1021/ja066563d.

(25) Chen, M. S.; White, M. C. A Sulfoxide-Promoted, Catalytic Method for the Regioselective Synthesis of Allylic Acetates from Monosubstituted Olefins via C-H Oxidation. *J. Am. Chem. Soc.* **2004**, 126, *5* , 1346–1347. https://doi.org/10.1021/ja039107n.

(26) Fraunhoffer, K. J.; White, M.C. Syn-1,2-Amino Alcohols via Diastereoselective Allylic C-H Amination. *J. Am. Chem. Soc.* **2007**, *129* (23), 7274–7276. https://doi.org/10.1021/ja071905g.

(27) Young, A. J.; White, M.C. Catalytic Intermolecular Allylic C-H Alkylation. *J. Am. Chem. Soc.* **2008**, *130* (43), 14090–14091. https://doi.org/10.1021/ja806867p.

(28) Vemula, S. R.; Kumar, D.; Cook, G. R. Palladium-Catalyzed Allylic Amidation with N-Heterocycles via Sp^3 C-H Oxidation. *ACS Catal.* **2016**, *6* (8), 5295–5301. https://doi.org/10.1021/acscatal.6b01818.

CHAPTER 3. FUNCTIONALIZATION OF INDOLE AT THE C2 POSITION FOR C-N BOND FORMATION VIA METAL CATALYSIS

3.1. Introduction

Much of the worked discussed so far focuses heavily on 4(3H)-Quinazolinone. Chapter 3 will transition into discussing indole. Indole is a nitrogen containing heterocycle which is a privileged structure in medicinal chemistry[1,2,3]. Direct functionalization of the indole scaffold is a research topic of much interest in organic synthesis due to the advantages in late-stage functionalization. One of the challenges in direct indole functionalization is selectivity. The indole ring is most reactive at the C3 position, and that is where most reports are focused[4,5]. There are less reporting's for functionalization of the C2 position, and significantly less on the aryl backbone[6].

Various reports of different transition metals and directing groups have been shown to facilitate direct indole functionalization. Due to the high reactivity of the C3 position C-H bond, harsh reaction conditions and expensive metals are often used to selectively functionalize the C2 position. In addition to the over complex reaction conditions necessary to functionalize the C2 position, a noticeable lack of C-N bond formation reactions is observed in the literature using transition metals.

3.2. Transition Metal Catalyzed C2 Functionalization of Indole

Though the arylation of the C2 position has been well researched amination at the C2 position remains underdeveloped. Li, and coworkers reported Rh(III) catalyzed approach (Scheme 3.1) utilizing a pyrimidine directing group (**3.01**) to aminate the C2 position with sulfonyl azides (**3.02**) as the aminating source[7] resulting in the C2 aminated product (**3.03**). The use of N-pyrimidine directing groups is a common methodology use in indole C2 amination.

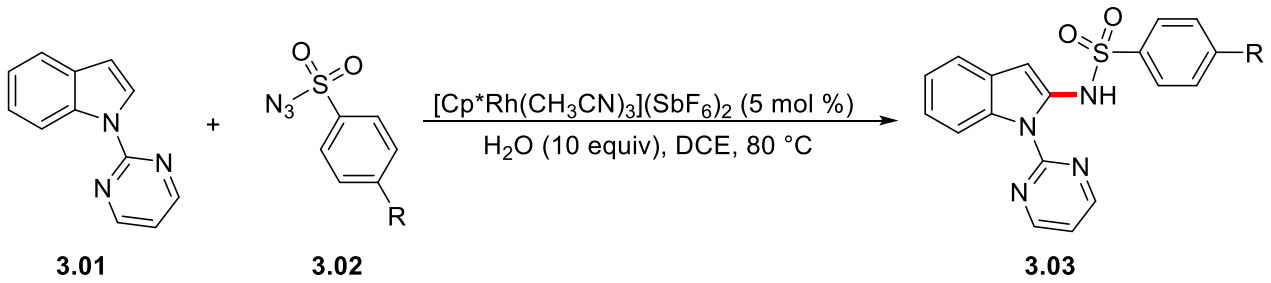

3.01 **3.02** **3.03**

Scheme 3.1: Rh(III) catalyzed C2 functionalization utilizing pyrimidine directing groups.

In 2014, Kanai and coworkers reported cobalt catalysts over rhodium which is a significantly a more sustainable option (Scheme 3.2). N-pyrimidyl directing groups (**3.01**) were used in conjunction with [Cp*Co(CO)I_2] pre-catalyst to generate Cp*Co^{III} *in-situ* via base activation[8]. They demonstrated the use of sulfonyl azides, and phosphoryl azides as the nucleophiles for C-H phosphoamidation (**3.04**) and sulphonamidation (**3.05**) of indoles. The reaction resulted in excellent yields but resulted in a poor substrate scope and steric limitations at the C3 position. Ackerman and coworkers reported a pyridine directing group variation using dioxazolones[9].

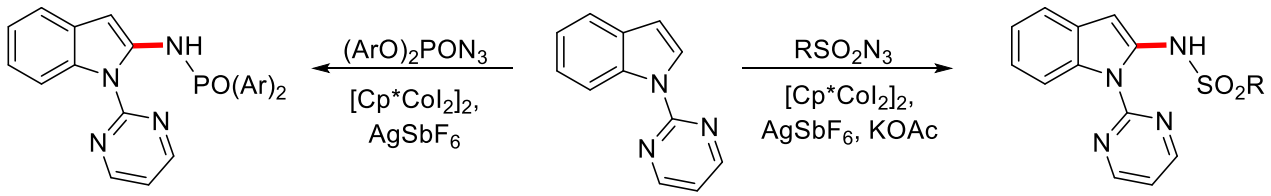

3.04 **3.01** **3.05**

Scheme 3.2: Cobalt catalyzed C2 functionalization utilizing a pyrimidine directing group.

Nagarajan and co-workers reported C2 functionalizing reaction that required the use of pre functionalized indole at the C2 and C3 position (**3.06**)[10,11]. The acyl group at the C3 position allowed for selective C2 coupling to produce amidated indole derivatives (**3.07**).

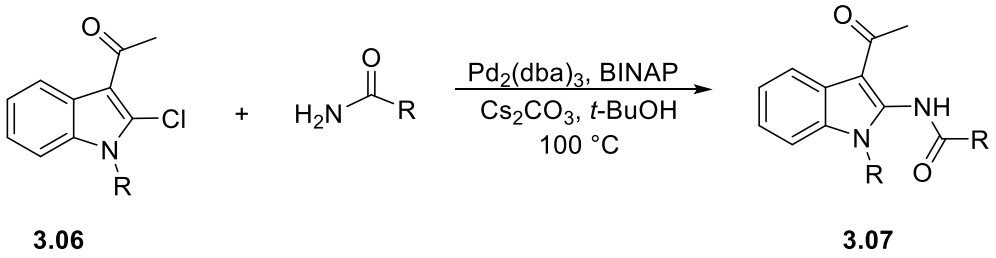

Scheme 3.3: Amidation of pre-functionalized indole via cross-coupling.

3.2.1. Palladium Catalyzed C2 Functionalization of 3-Allylindole

During our initial investigation regarding Pd-catalyzed allylic C-H oxidative amination reactions using terminal olefins and 4(3H)-Quinazolinone (Scheme 3.4), we were surprised by an unexpected product (**3.06**). Instead of the reaction resulting in the anticipated allylated product (**3.07**), we observed C2 amidation which allowed for the synthesis of fused heterocyclic structure **3.06**. The transformation was not observed when using White's protocol. The transformation was also not observed when non-functionalized indole was used, which suggest that the allyl group plays a role in the C2 amidation. We were intrigued by the unexpected product and decided to investigate further.

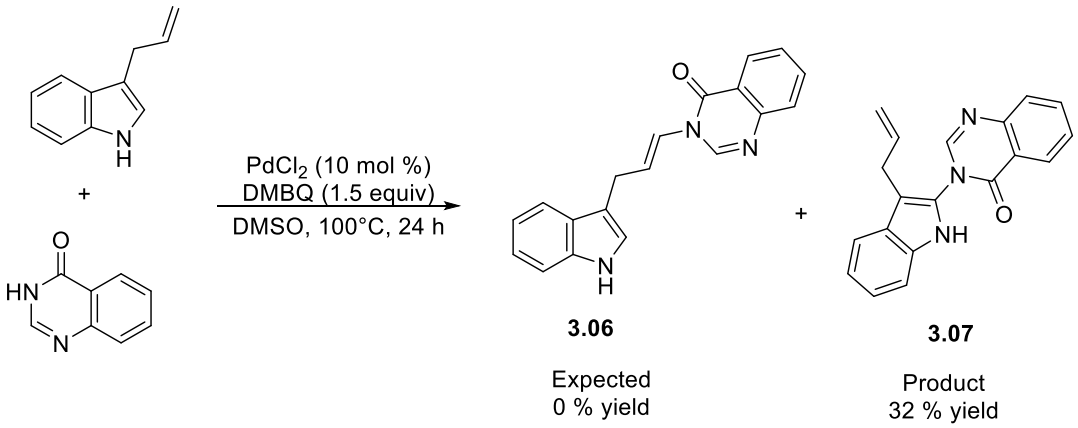

Scheme 3.4: Discovery of allyl direct C2 amidation reaction.

3.2.2. Allyl Directed Amidation of 3-Allylindole via Palladium and Nickel

Knowing that amination reactions of indole are rare, the reaction was investigated further. Screening of various palladium salts revealed that ligated palladium salts had detrimental effects on the reaction, and $PdCl_2$ proved the most effective. Solvent screening displayed that the addition of DCE alongside DMSO resulted in a more favorable reaction. With the addition of DCE, DMBQ was no longer necessary for the reaction. Screening of various metal salts other than palladium revealed $NiCl_2$ as a capable catalyst for the reaction giving **3.07** at a 52% yield. $NiCl_2$ could facilitate the reaction with superior yields compared to palladium (Scheme 3.5). $NiCl_2$ being a cheaper alternative and relatively less toxic provides advantages to the methodology and was further investigated.

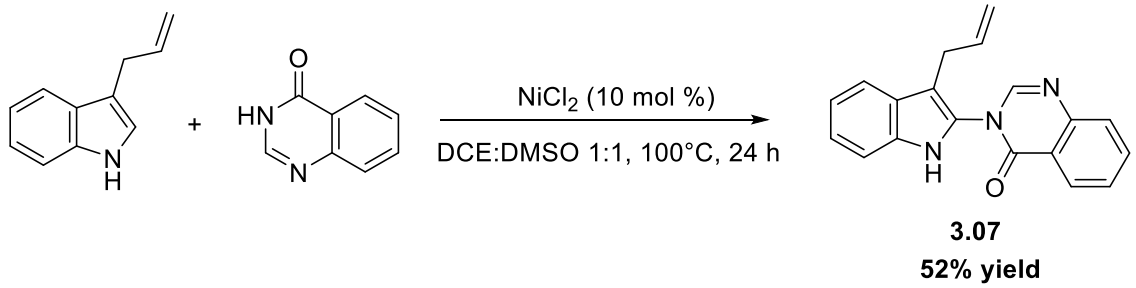

Scheme 3.5: Discovered $NiCl_2$ catalyzed C2 amidation of 3-Allylindole.

Further optimization of the reaction revealed that a higher concentration of DCE was beneficial to the reaction. Increasing the DCE ratio to 4:1 resulted in a 75% yield. Unfortunately, temperature, catalyst loading, and reaction time could not be decreased. That left the optimized conditions of the reaction to be $NiCl_2$ (10 mol %), DCE:DMSO (4:1), and a reaction time of 24 h at 100 °C (Scheme 3.06).

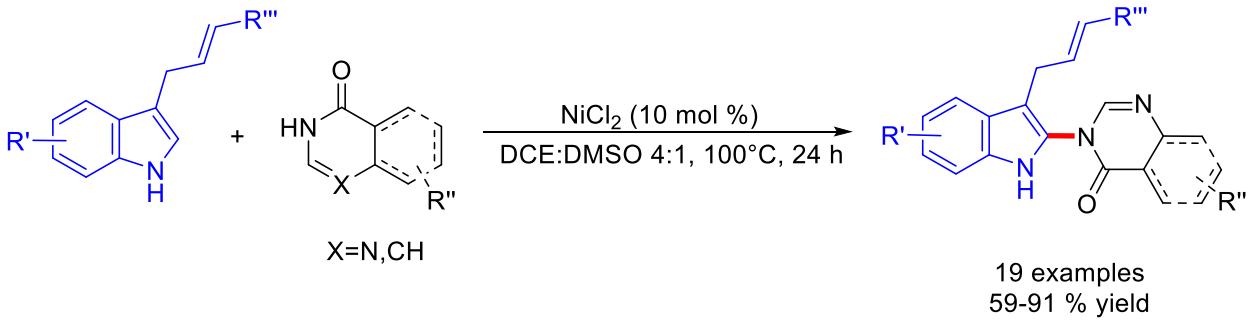

Scheme 3.6: $NiCl_2$ catalyzed C2 amidation of 3-Allylindole optimized.

With the optimized conditions in hand, the methodology was examined using various electron deficient, electron rich, and various C3 allyl substituted substrates to test the substrate scope. This resulted in good to excellent yields of all examined substrates. The N-heterocycle was expanded past 4(3H)-Quinazolinone to nucleophiles such as pyridines, pyridones, and pyrimidines. The reaction was capable of amidation of various C3 substituted indoles that contained π-bonds to give a variety of C3 substituted fused heterocycles (**3.08-3.11**). When 3-Methylindole was used, no reaction was observed (Scheme 3.7).

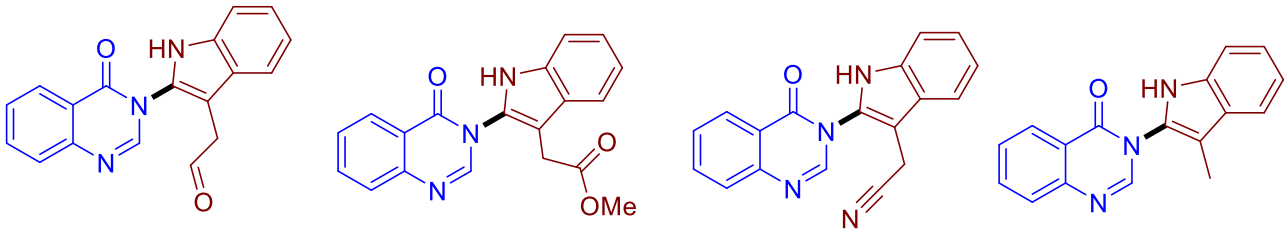

3.08 **Pd= 28%** **Ni=76%**

3.09 **Pd= 38%** **Ni=92%**

3.10 **Pd= 32%** **Ni=90%**

3.11 **Pd=NR** **Ni=NR**

Scheme 3.7: C3 substituted indole scope of established reaction.

3.2.3. Allyl Directed Amidation via $PdCl_2$/$NiCl_2$ Mechanism

Due to its reliance on π-bonds, the reaction was believed to be olefin directed. The metal is believed to coordinate to the olefin followed by C-H activation at the C2 position, in which

HCl is most likely expunged. This also results in a stable 5-member ring intermediate. Then followed by a nucleophilic attack on the metal, and reductive elimination resulting in the fused heterocycle product. The metal is believed to be oxidized by DCE which is demonstrated by the reaction's dependence on DCE and the fact that DMBQ is no longer needed (Scheme 3.8).

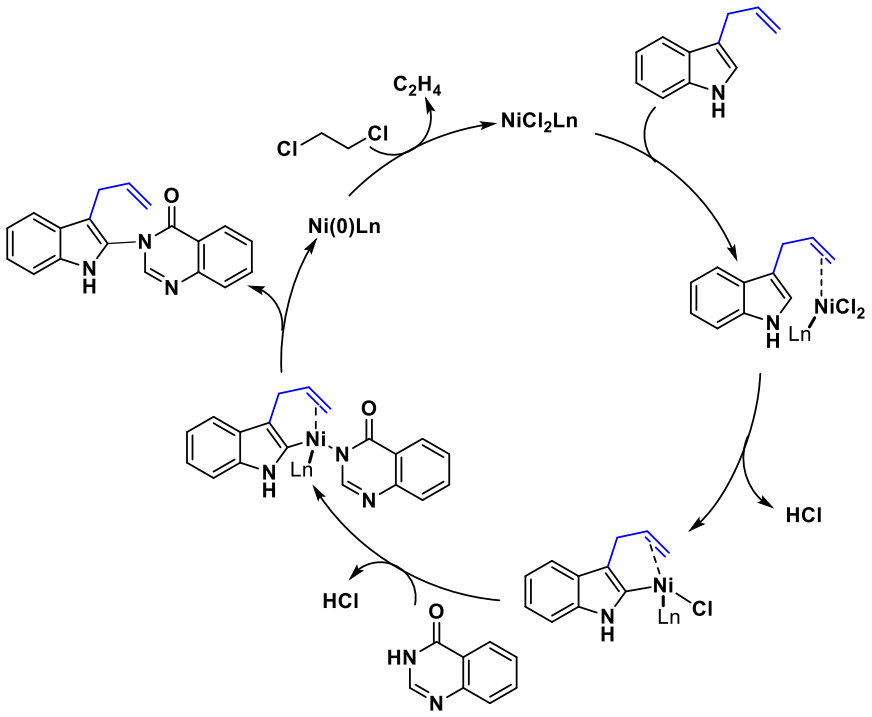

Scheme 3.8: Proposed reaction mechanism of $NiCl_2/PdCl_2$ mediated C2 indole functionalization.

3.3. C2 Functionalization of 3-Methylindole via Iron

During the screening process of the reaction, it was observed that iron salts could facilitate the reaction also. Iron being a naturally abundant, cheap, and green catalyst piqued our interest. Substrate screening revealed that iron was able to effectively cross couple a wider set of indole derivatives which included 3-Methylindole to give the product **3.12**.

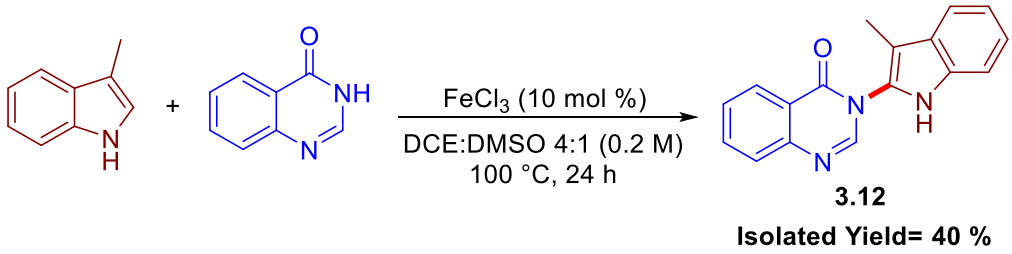

Scheme 3.9: Discovered $FeCl_3$ catalyzed reaction to yield **3.12**.

3.3.1. Reaction Optimization Iron Catalyzed C2 3-Methylindole Amidation

Initial screening of the reaction begun with the investigation of various metal salts. $PdCl_2$ and $NiCl_2$ were shown incapable of yielding the desired product (**3.15a**). Ruthenium, Indium, Bismuth, and iron salts did result in the desired product (Table 3.1).

Table 3.1: Effects of various metal salts on the coupling of 3-Methylindole with 4(3H)-Quinazolinone.

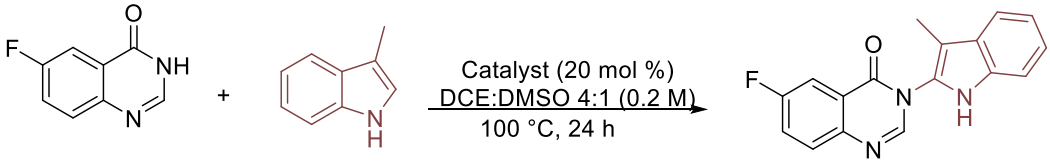

3.13a **3.14a** **3.15a**

Entry	Catalyst	Yield (%)
1	$PdCl_2$	0
2	$NiCl_2$	0
3	$FeCl_3$	73
4	$RuCl_3$	81
5	$InCl_3$	30
6	$InBr_3$	65
7	InF_3	42
8	$BiCl_3$	43
9	$BiBr_3$	46

Reaction conditions: 3.14a (0.2 mmol, 2.0 equiv) was treated with **3.13a** (0.1 mmol, 1.0 equiv) in the presence of different catalyst (20 mol %) in DCE:DMSO (0.2 M) at 100 °C for 24 h. Yield of **3.15a** quantified using F-NMR with DMSO-D6 and trifluoromethyl benzene internal standard. Reactions were done in duplicates or triplets.

Though many different metal salts were effective, the use of iron remained appealing. Iron salt screening revealed that $FeCl_3•6H_2O$ was a highly effective catalyst. This is theoretically due to the increased electrophilicity of the hydrate form (Table 3.2).

Table 3.2: Effects of various Iron salts on the coupling of 3-Methylindole with 4(3H)-Quinazolinone

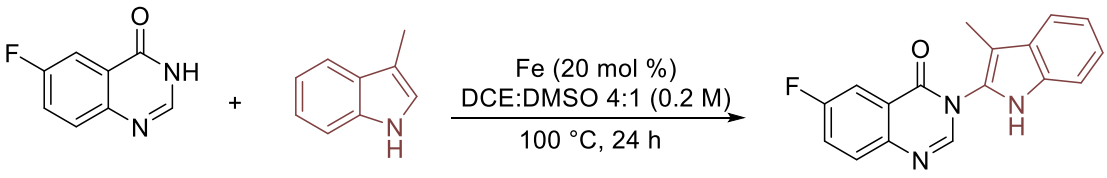

3.13a **3.14a** **3.15a**

Entry	Fe salt	Yield (%)
1	$FeCl_3$	74
2	$FeCl_2$	64
3	$Fe(OAc)_2$	11
4	$FeCl_3•6H_2O$	90
5	$Fe(acac)_2$	26
6	$FeCp_2$	75
7	$FeCp^*_2$	15
8	$FeSO_4•7H_2O$	63
9	$Fe(NO_3)•9H_2O$	33
10	$FeBr_3$	84

Reaction conditions: 3.14a (0.2 mmol, 2.0 equiv) was treated with **3.13a** (0.1 mmol, 1.0 equiv) in the presence of different Fe catalyst (20 mol %) in DCE:DMSO (0.2 M) at 100 °C for 24 h. Yield of **3.15a** quantified using F-NMR with DMSO-D6 and trifluoromethyl benzene internal standard. Reactions were done in duplicates or triplets.

It was shown that the use of $FeCl_3$ in tandem with H_2O as an additive successfully facilitated the reaction. This advantageous due to $FeCl_3•6H_2O$ being more expensive than $FeCl_3$ and having a shelf life from about 6-12 months. Adding H_2O as an additive makes the reaction more practical in terms of reaction execution and affordability (Table 3.3).

Table 3.3: Effects of water additive on the coupling of 3-Methylindole with 4(3H)-Quinazolinone.

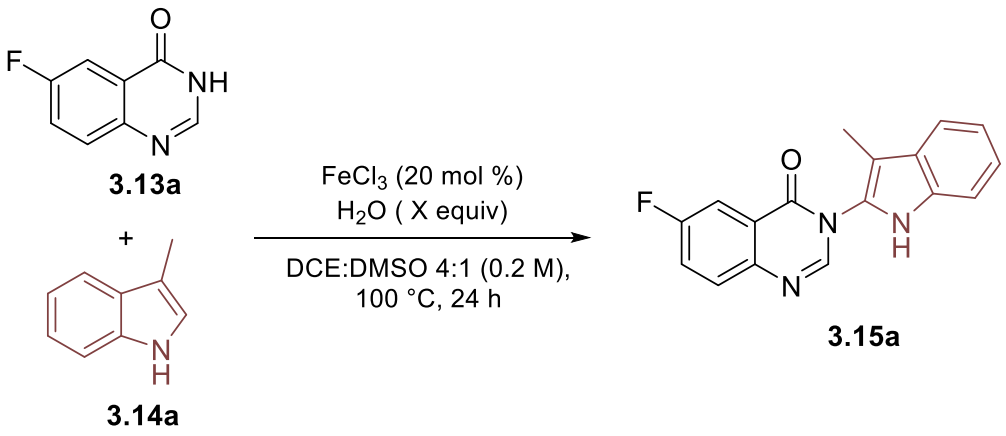

Entry	H_2O (equiv)	Yield (%)
1	1.0	71
2	2.0	91
3	3.0	79
4	4.0	70
5	12.0	58
6	24.0	28

Reaction conditions: 3.14a (0.2 mmol, 2.0 equiv) was treated with **3.13a** (0.1 mmol, 1 equiv) in the presence of $FeCl_3$ (20 mol %) and H_2O (equiv with respect to catalyst) in DCE:DMSO (0.2 M) at 100 °C for 24 h. Yield of **3.15a** quantified using F-NMR with DMSO-D6 with trifluoromethyl benzene as the internal standard. Reactions were done in duplicates or triplets.

Common ligands such as phenathroline, and bipyridines were used as an attempt to reduce catalyst loading. The use of ligands only had a marginal effect and was quickly abandoned (Table 3.4). The use of the $FeCl_3 \bullet 6H_2O$ proved much more effective as opposed to the ligands applied. Ligands can often make reaction cost high, so the removal of ligands is beneficial to our reaction.

Table 3.4: Effects of ligands on the coupling of 3-Methylindole with 4(3H)-Quinazolinone.

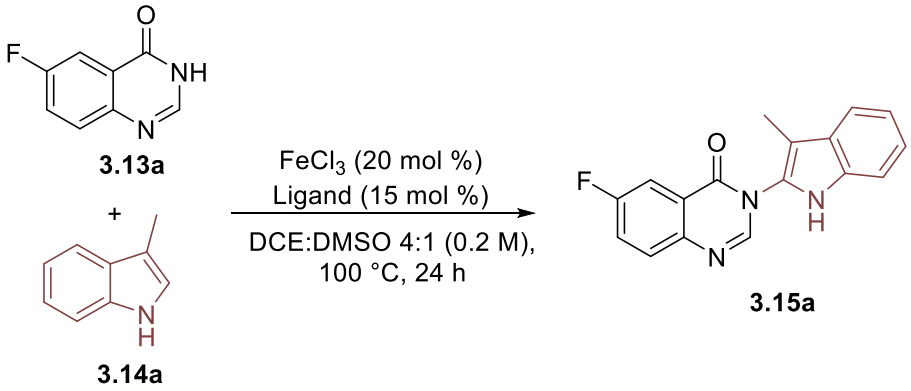

Entry	Ligand	Yield (%)
1	L1; 2,2′-Bipyridyl	63
2	L2; 4,4′-Di-tert-butyl-2,2′-dipyridyl	60
3	L3; 4-4′-Dimethoxy-2-2′-bipyridine	26
4	L4; 4-4′-Dinoyl-2-2′-bipyridine	61
5	L5; Bathophenanthroline	57
6	L6; 3,4,7,8-Tetramethyl-1,10 phenanthroline	62
7	L7; 1,9-Dimethyl phenanthroline	50
8	L8; Phenanthroline	63
9	No ligands	50

Reaction conditions: **3.14a** (0.2 mmol, 2.0 equiv) was treated with **3.13a** (0.1 mmol, 1.0 equiv) in the presence of $FeCl_3$ (20 mol %) and different ligands (15 mol %) in DCE:DMSO (0.2 M) at 100 °C for 24 h. Yield of **3.15a** quantified using F-NMR with DMSO-D6 and trifluoromethyl benzene internal standard. Reactions were done in duplicates or triplets.

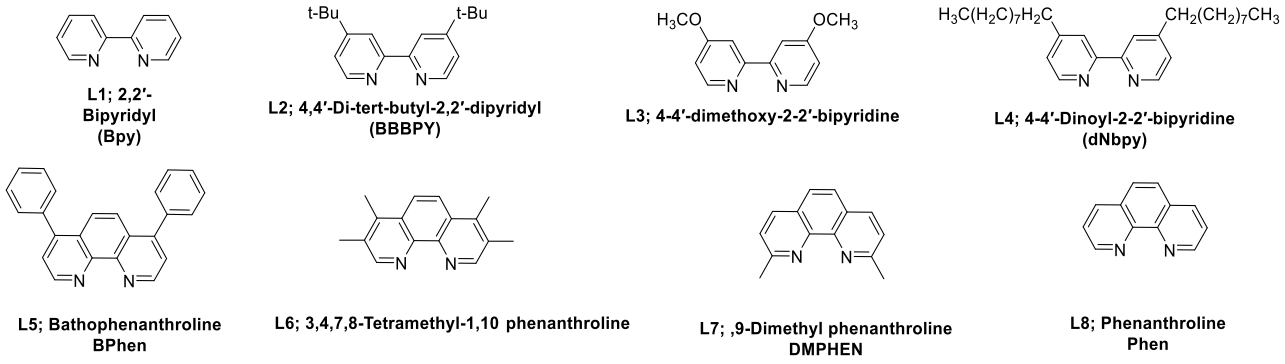

Figure 3.1: Various ligands applied on the coupling of 3-Methylindole with 4(3H)-Quinazolinone.

Solvent screening displayed that the reaction had a high dependence on DCE and DMSO. Various solvents were ineffective in facilitating the reaction resulting in no product (Table 3.5). However, when DCE and DMSO was used in a 4:1 ratio, the product was observed. The reaction was highly dependent on a 4:1 ratio as other ratio resulted in trace to no product. Pure DCE and DMSO were also ineffective.

Table 3.5: Effects of solvents on the coupling of 3-Methylindole with 4(3H)-Quinazolinone.

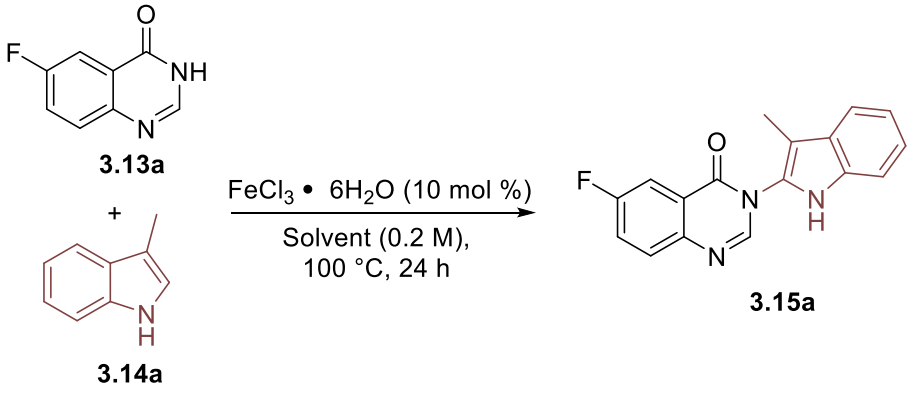

Entry	Solvent	Yield (%)
1	DCE	0
2	DMSO	0
3	DCE:DMSO 4:1	50
4	DCE:DMSO 3:2	Trace
5	DCE:DMSO 2:3	Trace
6	DCE:DMSO 1:4	Trace
7	Chlorobenzene	0
8	t-Amyl Alcohol	0
9	AcOH	0
11	Anisole	0
12	DMC	0
13	DMF	0
14	Toluene	0
15	1,4-Dioxane	0
16	Nitromethane	0

Reaction conditions: 3.14a (0.2 mmol, 2.0 equiv) was treated with **3.13a** (0.1 mmol, 1.0 equiv) in the presence of $FeCl_3 \bullet 6H_2O$ (10 mol %) and different solvents (0.2 M) at 100 °C for 24 h. Yield of **3.15a** quantified using F-NMR with DMSO-D6 and trifluoromethyl benzene internal standard. Reactions were done in duplicates or triplets.

Knowing that the reaction was highly dependent on DCE:DMSO ratio, the reaction was then screened for the effect of various concentrations. Increasing the molarity of the reaction resulted in significantly higher yields. Increasing the concentration from 0.2 M to 0.4 M resulted in a respectable 91% yield using only 10 mol % catalyst loading (Table 3.6).

Table 3.6: Effects of water additive on the coupling of 3-Methylindole with 4(3H)-Quinazolinone.

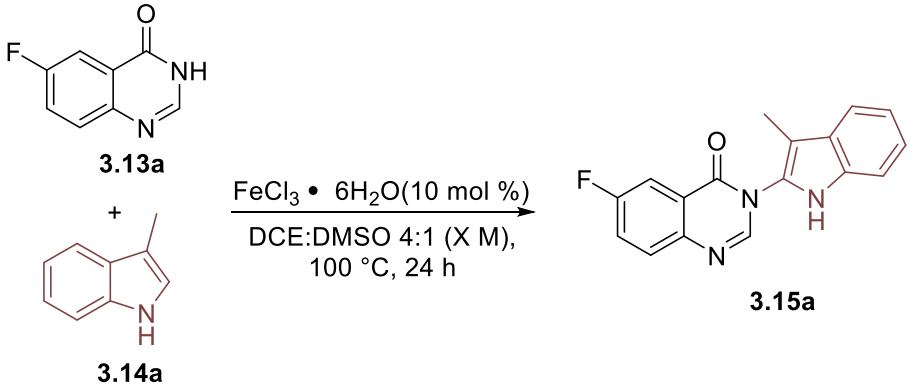

Entry	Solvent Concentration (M)	Yield (%)
1	0.1	Trace
2	0.2	50
3	0.3	>99
4	0.4	91

Reaction conditions: **3.14a** (0.2 mmol, 2.0 equiv) was treated with **3.13a** (0.1 mmol, 1 equiv) in the presence of $FeCl_3$•$6H_2O$ (10 mol %) and various solvent concentrations at 100 °C for 24 h. Yield of **3.15a** quantified using F-NMR with DMSO-D6 and trifluoromethyl benzene internal standard. Reactions were done in duplicates or triplets.

It was determined that the concentration of the substrate had a dramatic effect on the reaction's effectiveness (Table 3.7). Decreasing the amount of indole from 2.0 to 1.2 equiv decreased the reactions yield to as low as 40%. It is apparent that the reaction is highly dependent on high concentrations of indole to work effectively.

Table 3.7: Effects of 3-Methylindole concentration on the coupling of 3-Methylindole with 4(3H)-Quinazolinone.

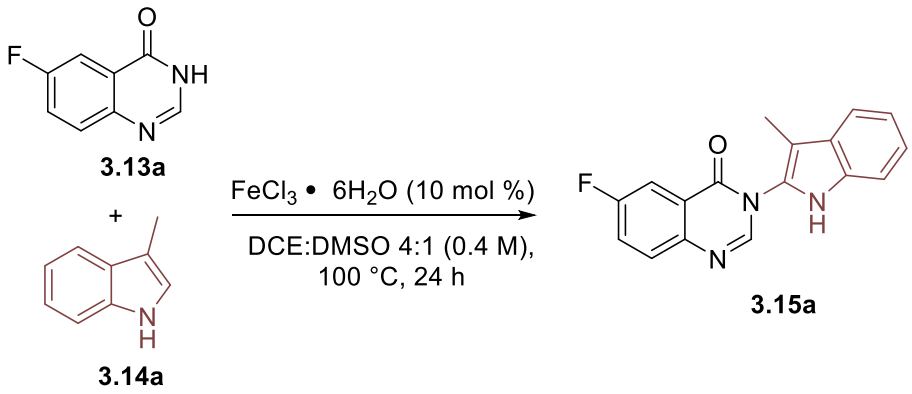

Entry	Indole (equiv)	Yield (%)
1	1.2	40
2	1.4	73
3	1.6	88
4	1.8	91
5	2.0	99

Reaction conditions: Various amounts of **3.14a** was treated with **3.13a** (0.1 mmol, 1.0 equiv) in the presence of $FeCl_3$•$6H_2O$ (10 mol %) in DCE:DMSO (0.4 M) at 100 °C for 24 h. Yield of **3.15a** quantified using F-NMR with DMSO-D6 and trifluoromethyl benzene internal standard. Reactions were done in duplicates or triplets.

Reduction of the reaction temperature resulted in a dramatic decrease in the yield (Table 3.8). It appears that the reaction was highly dependent on elevated temperatures. A 90 °C reaction temperature resulted in only trace yields for the reaction. After the temperature was lowered under 90 °C; no product was detected at all.

Table 3.8: Effects of temperature on the coupling of 3-Methylindole with 4(3H)-Quinazolinone.

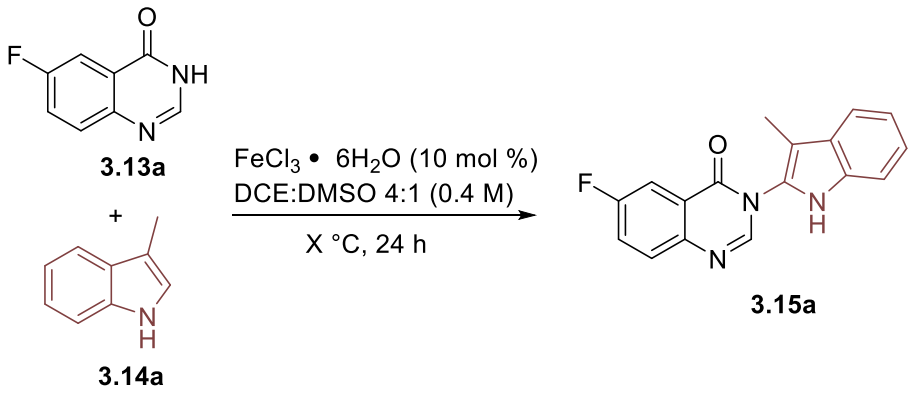

Entry	Temperature (°C)	Yield(%)
1	100	94
2	90	Trace
3	80	0
4	70	0
5	60	0
6	50	0

Reaction conditions: 3.14a (0.18 mmol, 2.0 equiv) was treated with **3.13a** (0.1 mmol, 1.0 equiv) in the presence of $FeCl_3$•$6H_2O$ (10 mol %) in DCE:DMSO (0.4 M) at various temperatures for 24 h.Yield of **315a** quantified using F-NMR with DMSO-D6 and trifluoromethyl benzene internal standard. Reactions were done in duplicates or triplets.

The reaction time was also examined, revealing that the reaction required at least 16 hours to result in yields above 90% (Table 3.9). Dropping the reaction time from 24 h to 20 h resulted in a slightly lower yield. Though 24 hours was optimal, 16 hours was still sufficient for a good yield.

Table 3.9: Effects of time on the coupling of 3-Methylindole with 4(3H)-Quinazolinone.

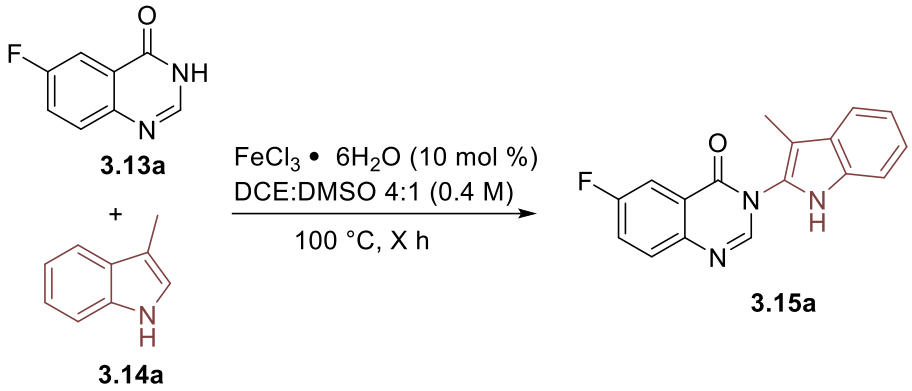

Entry	Reaction time (h)	Yield (%)
1	6	23
2	12	68
3	16	91
4	18	94
5	20	94
6	24	>99

Reaction conditions: 3.14a (0.18 mmol, 1.8 equiv) was treated with **3.13a** (0.1 mmol, 1.0 equiv) in the presence of $FeCl_3 \bullet 6H_2O$ (10 mol %) and different ligands (15 mol %) in DCE:DMSO (0.4 M) at 100 °C for 24 h. Yield of **3.15a** quantified using F-NMR with DMSO-D6 and trifluoromethyl benzene internal standard. Reactions were done in duplicates or triplets.

3.3.2. Substrate Scope of Iron Catalyzed C2 3-Methylindole Amidation

The substrate scope of the reaction was then screened to get an idea of what types of indoles were suitable for the reaction (Scheme 3.10). Screening various 3-substituted indole determined that C3 alkylated indoles at worked excellent for this reaction (**3.18a-i**). The reactions worked well for non-sterically hindered C3 substituted indoles. However, it can be observed that bulky groups such as 3-^{t}butyl and 3-Phenylindole (**3.18g-3.18h**) were not as effective.

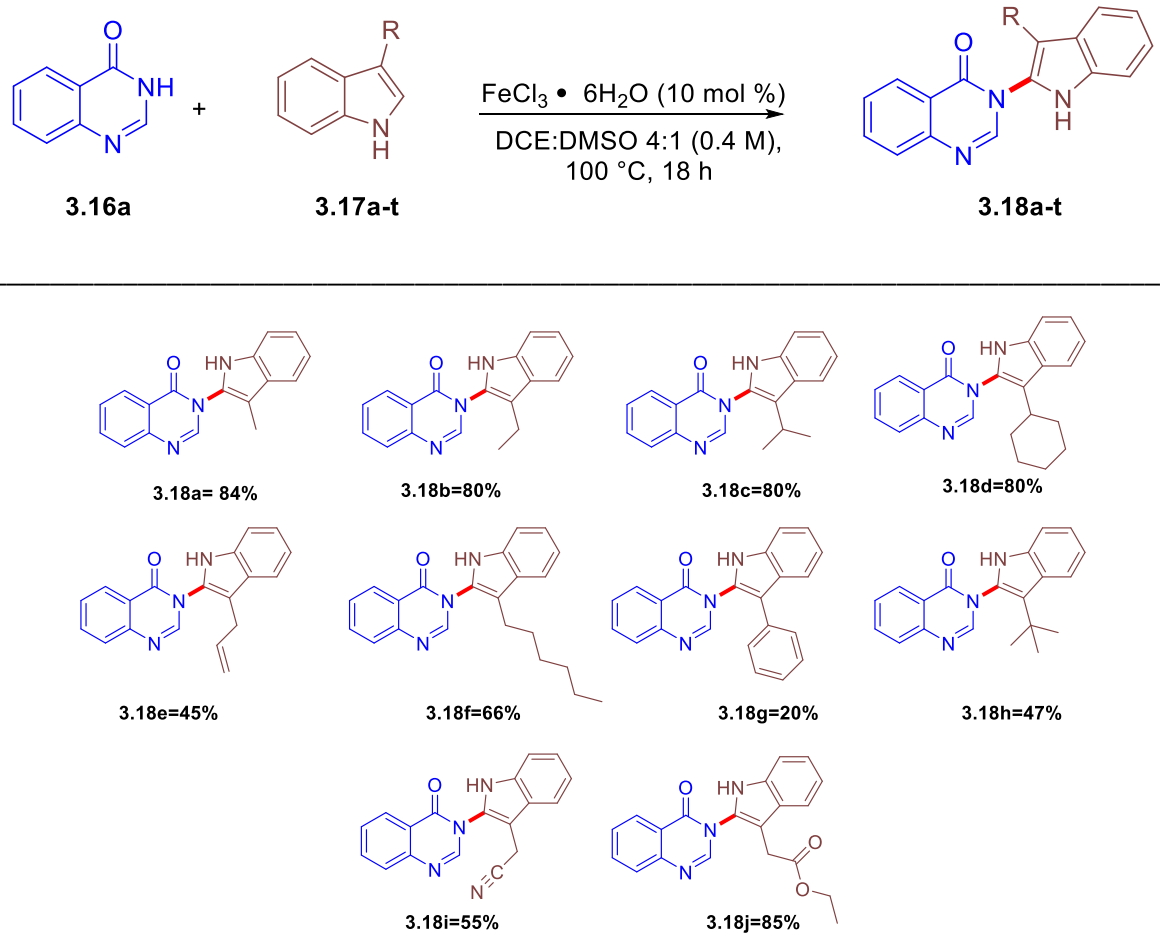

Scheme 3.10: Substrate Scope of C3 functionalized indoles.

Not surprisingly, substrates such as non-functionalized indole, and 7-azaindole failed as well (**3.18k, 3.18p**). Unfunctionalized indole in notably hard to selectively functionalize, due to the high reactivity of the C3 position. Substrates containing EWG also were not functionalized under these reaction conditions (Scheme 3.11). Sadly, tryptophan and its derivatives showed no product formation (**3.18q-t**).

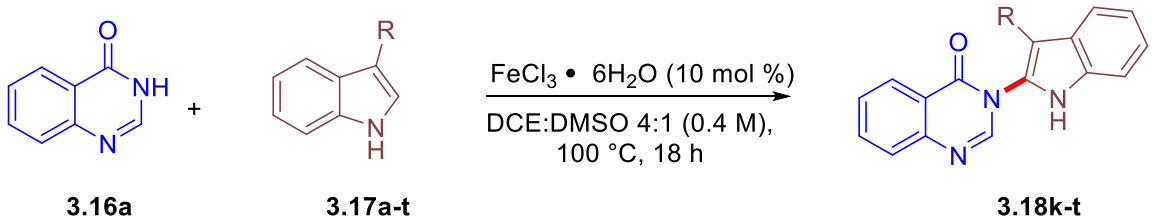

3.16a **3.17a-t** **3.18k-t**

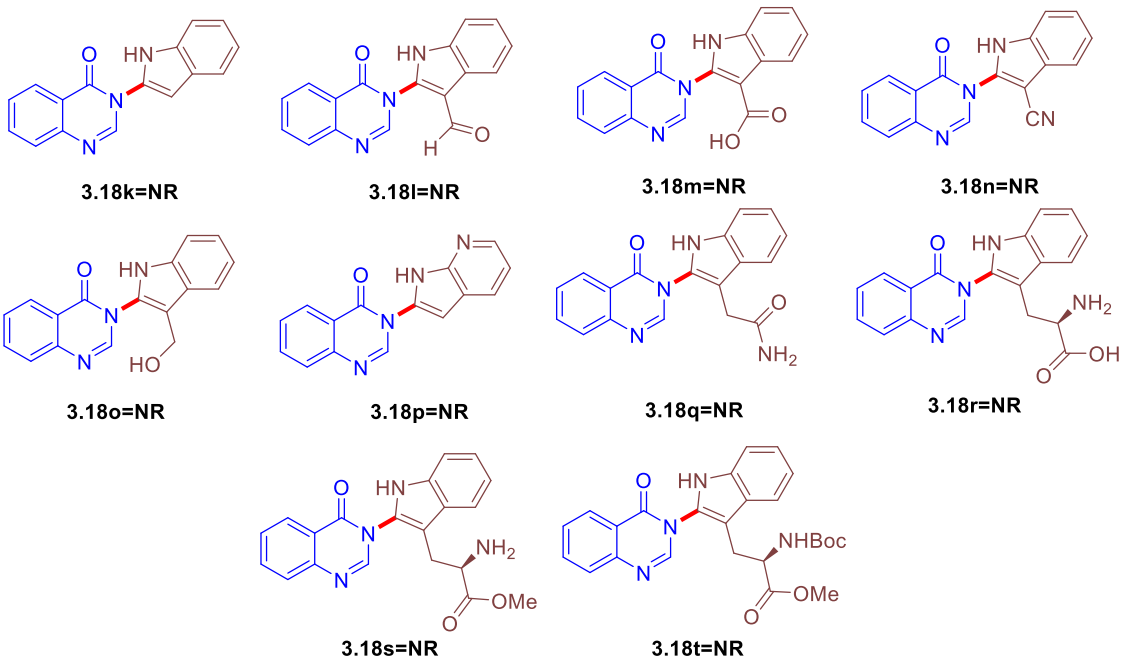

Scheme 3.11: Indole substrate that resulted in no reaction in the outlined reaction.

The reaction was effective on various N-heterocycles such as pyridones, and pyridines and 4(3H)-one derivatives (**3.15a-j**). As anticipated, the reaction was shown to be more effective on electron rich heterocycles than electron poor heterocycles. This was to be expected since the N-heterocycle most likely acts as the nucleophile.

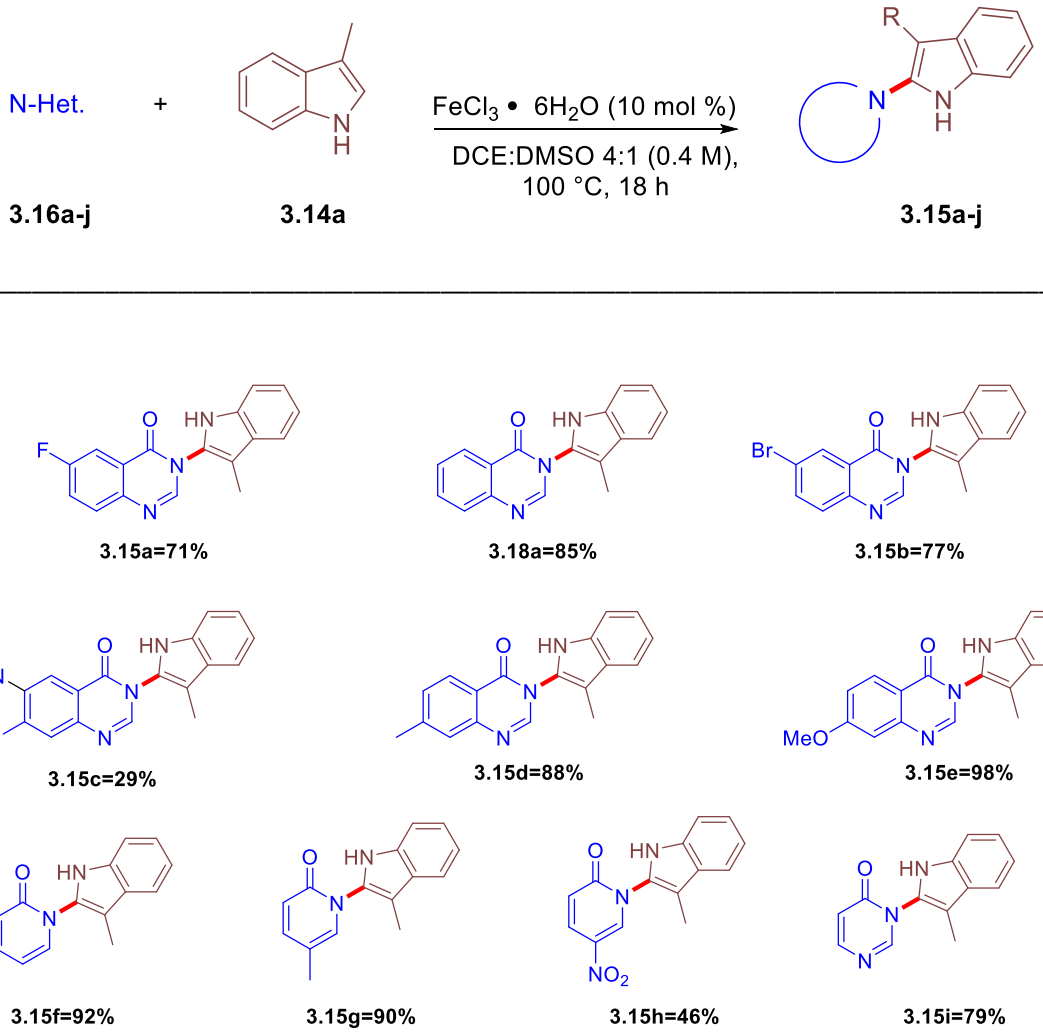

Scheme 3.12: Substrate scope of various tautomerizable N-heterocycles under outlined reaction conditions.

3.3.3. Mechanistic Investigation of 3-Methylindole C2 Functionalization

Optimization of reaction conditions gave insight into some of the possible mechanisms, however additional experiments were done to help elucidate the most likely mechanism. Mechanism determination was begun by researching the literature to help determine the possibilities[12]. It was then followed up by control experiments or literature research that would give evidence of whether that reaction mechanism is plausible.

N-iodosuccinimide (NIS) has been reported as a reagent for amidation of 3-Methylindole. Nagarajan and coworkers have reported using NIS to functionalize the C2 position of 3-Methylindole with 4(3H)-Quinazolinone[13]. The electrophilic NIS reagent reacted at the C3 position which formed a indoline intermediate (**3.19**). This allowed 4(3H)-quinazoline to attack the C2 position forming Indolylquinazolinone (**3.20**).

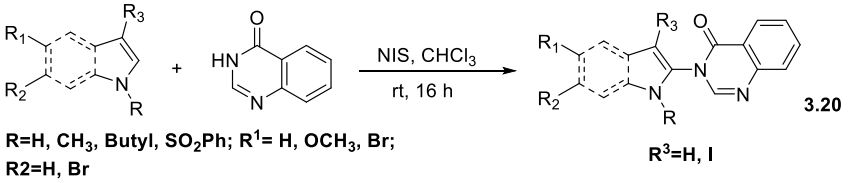

Scheme 3.13: NIS mediated amidation of 3-Methylindole.

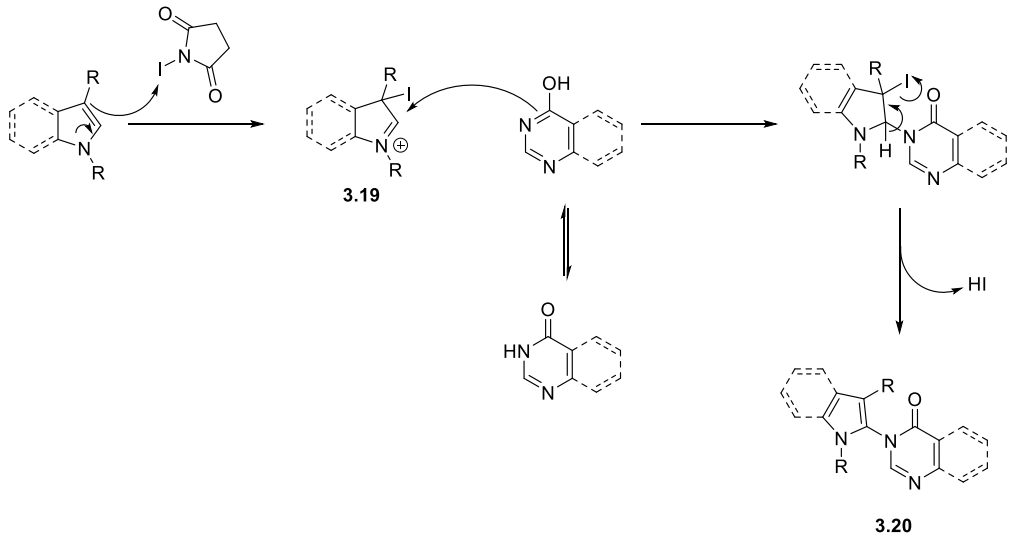

Scheme 3.14: NIS mediated amidation of 3-Methylindole proposed mechanism.

We initially thought that the reaction may undergo a similar mechanism (Scheme 3.14). However, that would require for Fe to undergo a two-electron transfer to form Fe^{I}. The literature shows that though Fe^{I} pathways are possible, but highly unlikely under these conditions. Formation of Fe^{I} has only been reported in the literature under more complex reaction conditions using complex ligands that act as radical sinks to promote two-electron process to occur. We can comfortably say that this mechanism is highly unlikely.

Rampon and co-workers reported a similar mechanism where $FeCl_3$ was used under similar conditions to functionalize the C3 position of indole with organoselenium or sulfur reagents (Scheme 3.15)[14]. Though the position of the indoles differs in their work, C2 functionalization was found when 3-Methylindole was used. The author suggested a Planchar rearrangement.

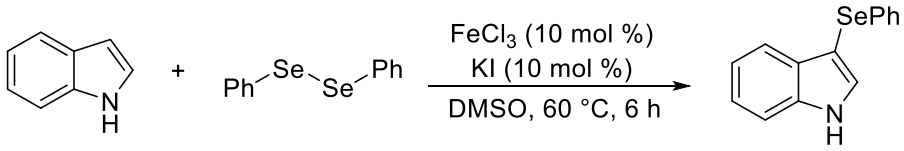

Scheme 3.15: Fe(III)-Catalyzed Direct C3 Chalcogenylation of Indole.

The use of potassium salts in this reaction allowed for the formation of iodide, KCl, $FeCl_2$, and Fe_2O_3 in equilibrium. The iodide was key for activating the organo-selenium reagent (scheme 3.16). The organoselenium intermediate formed coordinating to the iron (**3.21**) formed an electrophilic intermediate which reacted with at the C3 position of the indole (**3.22**). Re-aromatization allowed for the formation of the final product (**3.23**).

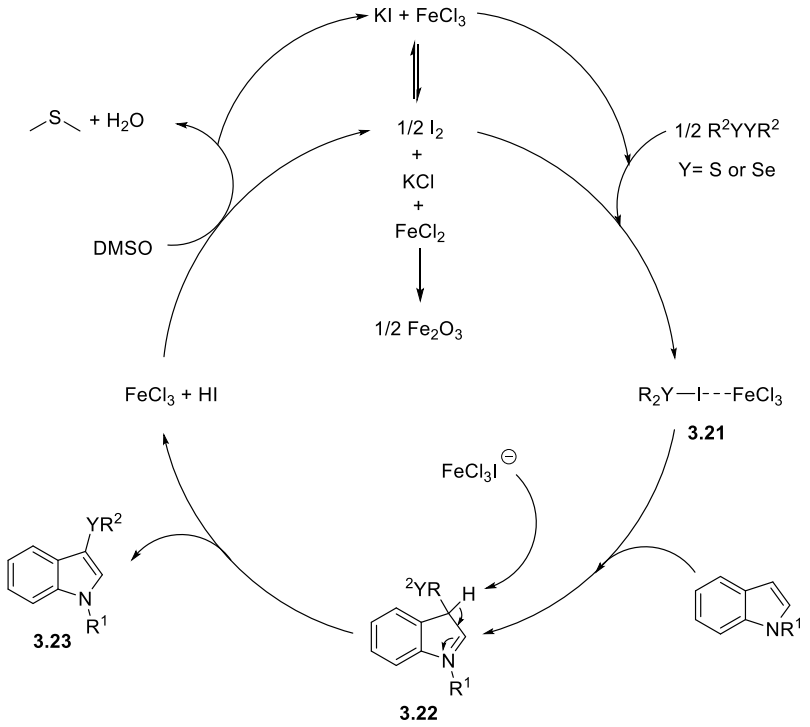

Scheme 3.16: Fe(III)-Catalyzed Direct C3 Chalcogenylation proposed mechanism.

With knowledge of the mechanism suggested by Rampon and co-workers, control experiments were done to test if the reaction mechanisms are similar (Table 3.10). Unlike the reaction designed by our group, their reaction requires no DCE to facilitate the reaction. Their reaction was highly dependent on the potassium salts, which may play a similar role as DCE. Our reaction was done using various potassium salt which resulted in no product. Additionally, no product was observed when using the exact conditions same conditions reported by Rampon (Table 3.10, entry 5), suggesting that a similar mechanism may not be occurring.

Table 3.10: Effects of Potassium salts on Fe(III) catalyzed C2 amidation of 3-Methylindole.

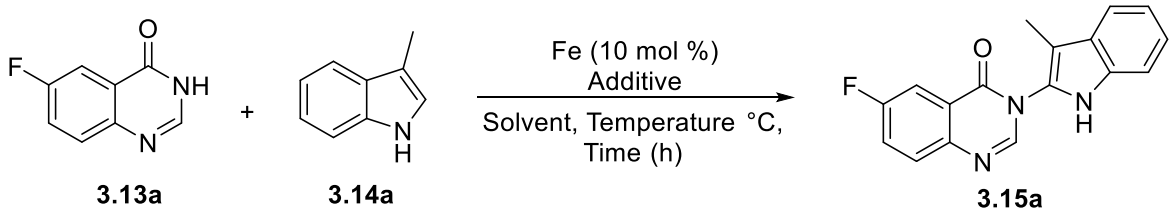

Entry	Catalyst	Additive (mol %)	Time (h)	Temp. (°C)	Yield (%)
1	$FeCl_3$ x 6 H_2O	KF(30)	18	100	NR
2	$FeCl_3$ x 6 H_2O	KCl(30)	18	100	NR
3	$FeCl_3$ x 6 H_2O	KBr(30)	18	100	NR
4	$FeCl_3$ x 6 H_2O	KI(30)	18	100	NR
5	$FeCl_3$	KI(30)	3	60	NR

Reaction conditions: 3.13a (0.18 mmol, 1.8 equiv) was treated with **3.14a** (0.1 mmol, 1.0 equiv) in the presence of $FeCl_3$•$6H_2O$ (10 mol %) DMSO (0.4 M. Yield of **3.15a** quantified using F-NMR with DMSO-D6 and trifluoromethyl benzene internal standard. [b]Product detected through TLC. Reactions were done in duplicates or triplets.

When 3-Methylindole was used for chalcogenylation (Scheme 3.15); C2 functionalization was observed. The author suggested a Planchar rearrangement. The Planchar rearrangement is driven by the formation of a stable tertiary carbocation intermediate that forms upon rearranging from the C3 position to the C2 position (Scheme 3.17)[15]. The possibility of a Planchar rearrangement was investigated that would go through a mechanism similar (Scheme 3.18).

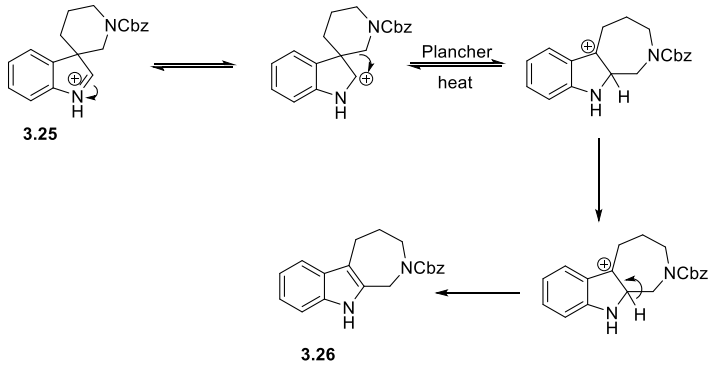

Scheme 3.17: Example of a spirocyclic indole undergoing a Planchar rearrangement.

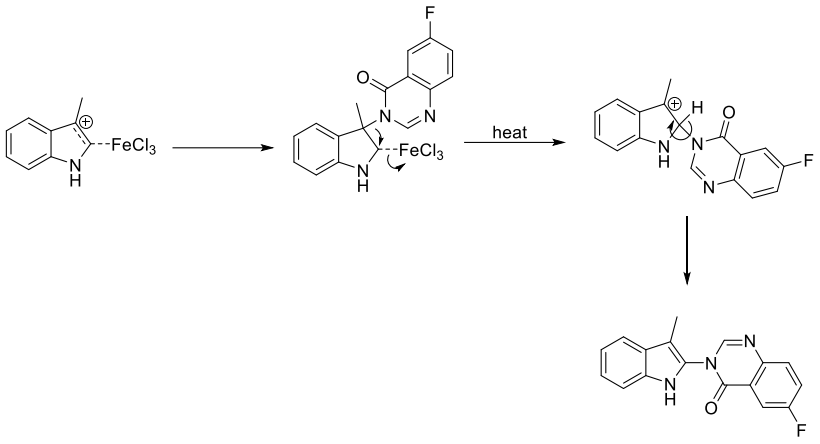

Scheme 3.18: Possible Planchar rearrangement of our reaction.

Ovola-Cintron and co-workers demonstrated the observation of a Planchar rearrangement occurring in a reaction of a spirocyclic indole (**3.25**) synthesized through cyclization from the corresponding hydrazone (**3.24**) (Scheme 3.17). They were able to observe the formation of the fused indole ring by monitoring the reaction via TLC and GC-MS. The reaction showed over the course of 24 h that the reaction was completely converted to the fused indole at room temperature. Hours 1-22.5 showed evidence of **3.24** slowly converting to the fused indole (**3.26**). When the reaction was done at room temperature, it was observed that the rearrangement was heavily influenced by heat as the reaction was complete within an hour when heated.

Table 3.11: Tracking of Planchar rearranged product (**3.26**) and spirocyclic indole (**3.25**).[15]

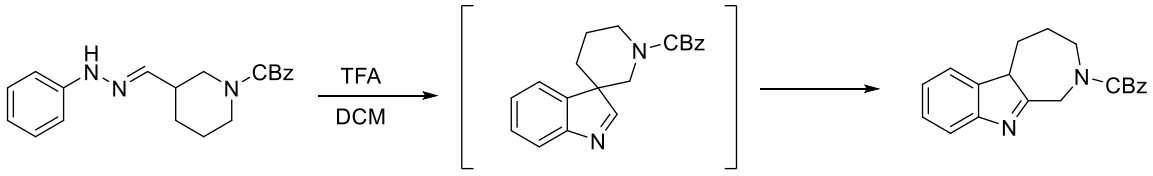

Hydrazone (3.24) **Spiroindole (3.25)** **Fused Indole (3.26)**

Entry	Time	Hydrazone 3.24 (%)	Spiroindole 3.25 (%)	Fused Indole 3.26 (%)
1	0	100	0	0
2	1	42	43	15
3	4	0	49	57
4	6.5	0	32	68
5	8.5	0	29	71
6	22.5	0	9	91
7	24	0	0	100

Applying the same strategy, resulted in no observation of C3 functionalized indole in our reaction. When the reaction was run at room temperature, no product was observed. When the reaction was done at (100 °C, the only observed product was the C2 functionalized product. No C3 functionalized product was observed which is evidence that no rearrangement is occurring.

Table 3.12: Control experiment for formation of C3 functionalized 3-Methylindole (**3.27**).

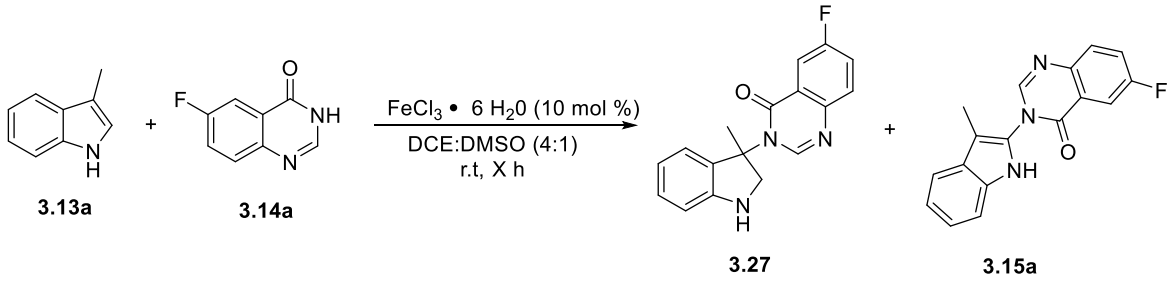

3.13a + **3.14a** → **3.27** + **3.15a**

Time (h)	4(3H)-Quinazolinone (3.14a)	C3 amidation product (3.27)	C2 amidation product (3.15a)
6	100	0	0
12	100	0	0
18	100	0	0
24	100	0	0

Reaction conditions: 3.13a (0.18 mmol, 1.8 equiv) was treated with **3.14a** (0.1 mmol, 1.0 equiv) in the presence of $FeCl_3 \bullet 6H_2O$ (10 mol %) in DCE:DMSO (0.4 M) at 100 °C from 6-25 hr. Yield of **3.27 and 3.15a** quantified using F-NMR with DMSO-D6 and trifluoromethyl benzene internal standard. Product detected through TLC. Reactions were done in duplicates or triplets.

Further research into the possible mechanisms revealed that 3-Methylindole has a unique reactivity and is susceptible to oxidative coupling by one electron oxidants (Scheme 3.19). The first study from 1957 revealed that 3-Methylindole reacted with $FeCl_3$ results in a oxidatively coupled dimeric white crystal (**3.28**)[16]. This was also demonstrated by Tsuji and coworkers in 1981 where they detected the same oxidatively coupled product by reaction the 3-Methylindole using $Cu(OMe)_2$, however they suggested a different structure for the oxidatively coupled product. (**3.30**) [17]. It's suggested that 3-Methylindole undergoes single electron transfer to form a radical at the C3 position which allows for the formation of an indole dimer (**3.29**). The dimer then undergoes oxidation to form the oxidatively coupled indole product. Sayre and coworkers reported similar findings when they synthesized the 3-Methylindole dimer (**3.29**) using horseradish peroxidase under anaerobic conditions and reported a structurally corrected

oxidatively coupled dimer product (**3.31**). In addition, they reported a reasonable mechanism for the oxidation of the dimer (Scheme 3.19).

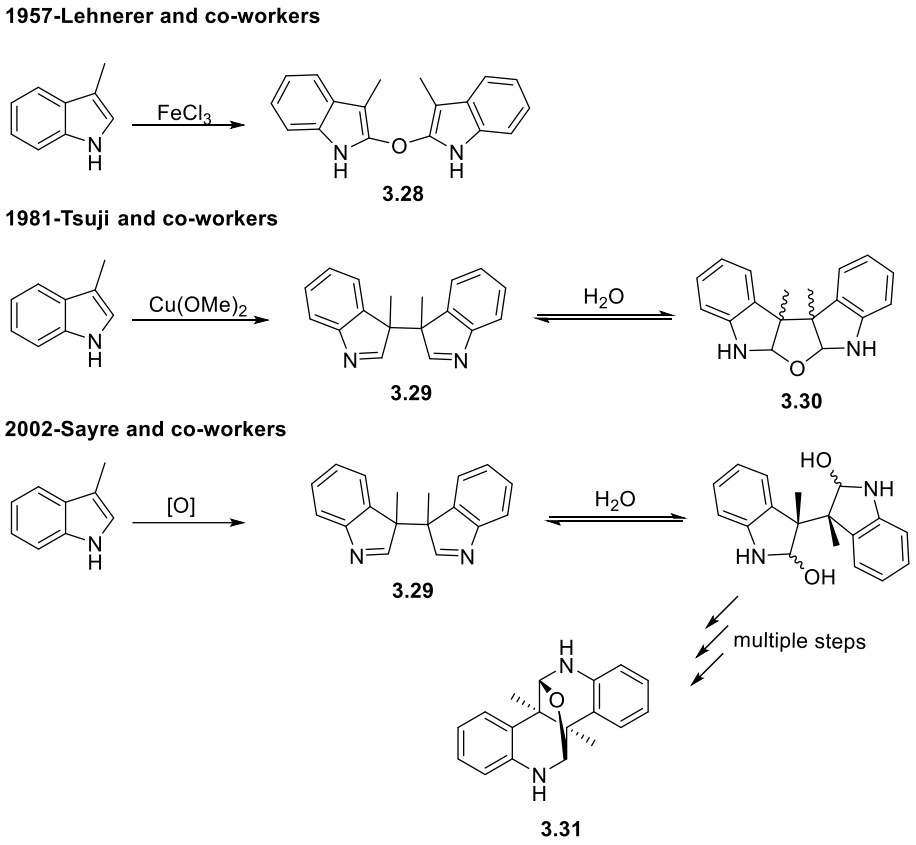

Scheme 3.19: 3-Methylindole oxidative coupling through indole dimerization.

The proposed reaction mechanism is like Sayre's mechanism. The indole undergoes SET catalyzed by the iron which forms a radical at the C3 position. The indole then dimerizes forming a 3-Methylindole dimer (**3.29**), which then undergoes nucleophilic attack at the C2 position. This is then followed by a re-aromatization step that forms the fused heterocycle product (**3.32**). Then DCE works to regenerate the iron catalyst through a SET mechanism, which reforms Fe^{III} (Scheme 3.20).

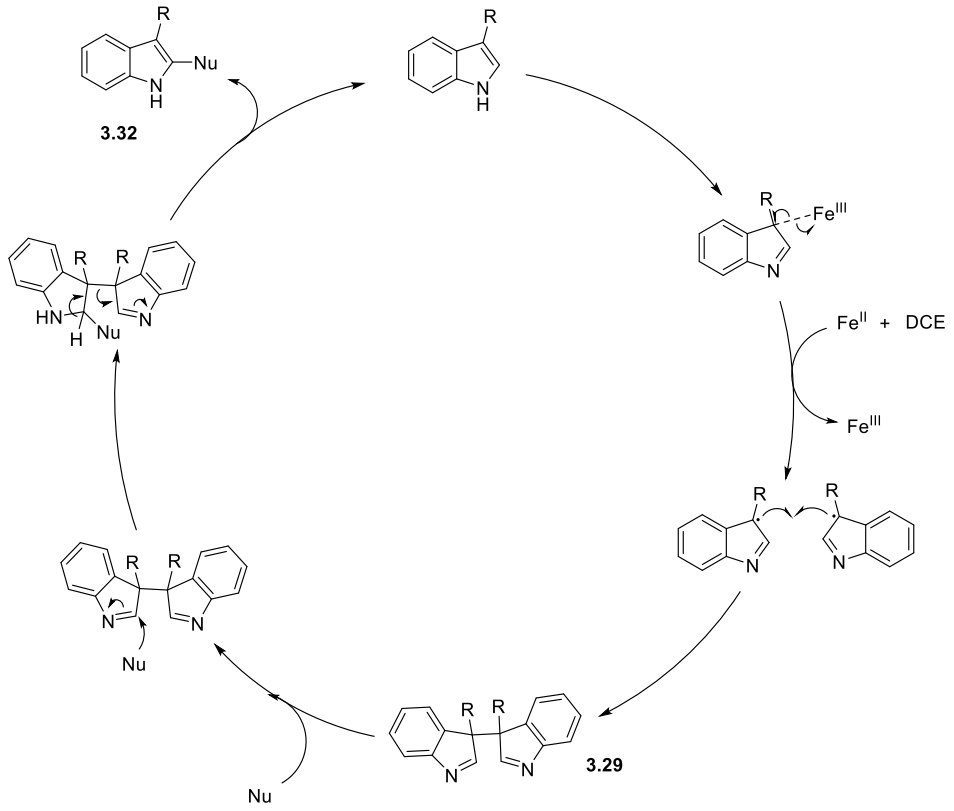

Scheme 3.20: Proposed reaction mechanism of iron catalyzed C2 amidation.

To help elucidate the mechanism further, DCE was removed from the reaction and replaced with $AgSbF_6$ which is known to act as an oxidant[18]. The absence of DCE resulted in no product formation. In the presence of $AgSbF_6$, a 61% yield was observed using solely DMSO as the solvent, which may indicate DCE acting as an oxidant[19,20] (Scheme 3.21). Lastly, the use of the radical scavenger TEMPO resulted in no product formation which is evidence of SET mechanism.

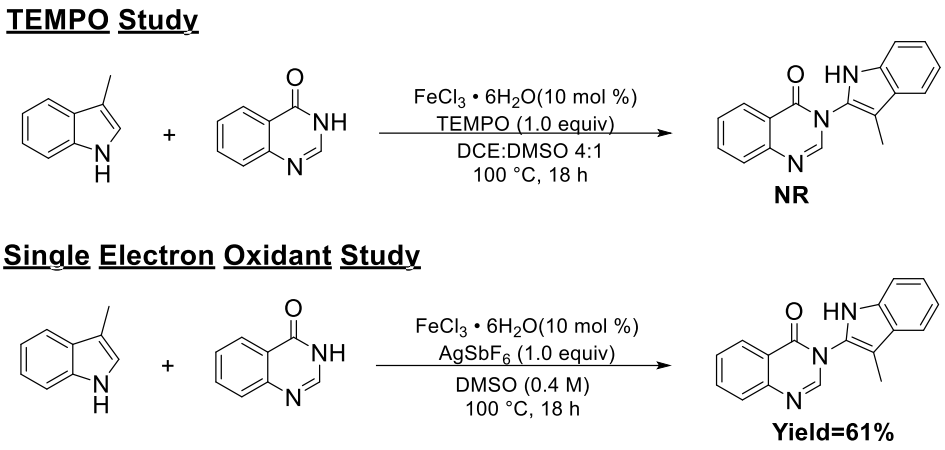

Scheme 3.21: Control experiments using radical scavenger (TEMPO) and an oxidant ($AgSbF_6$).

3.3.4. Future Direction

Future directions would include expanding the range of nucleophiles to non-tautomerizable N-heterocycles. Incorporation of other N-heterocycles may require the addition of a base, depending on the relative pka. Advantage of tautomerizable N-heterocycles is that bases aren't needed due to the presence of the enol. Use of N-heterocycles like morpholine, piperidine, pyrroles, or even nucleobases could yield promising structures.

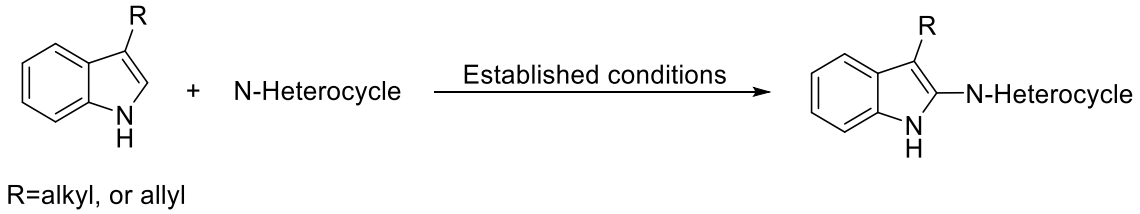

Scheme 3.22: Expansion of the N-heterocycle substrate.

Another direction would be to expand to azaindole derivatives. Azaindole is like indole rings but contain an electron deficient pyridine ring. Since azaindole is electron deficient, C3 and C2 become significantly less reactive. According to the literature, functionalization of the azaindole ring is difficult and therefore not much exist in the literature for functionalization.

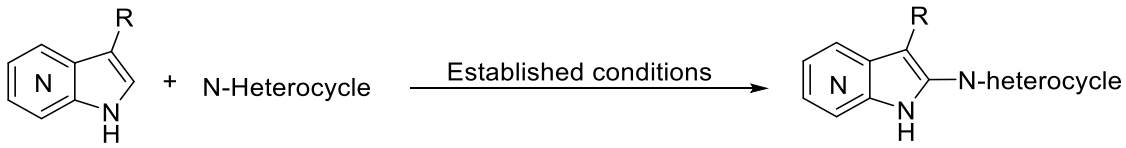

Scheme 3.23: Proposed C2 functionalization of azaindole.

3.4. Thoughts and Conclusion

In conclusion, we have reported a novel method for the synthesis of fused N-heterocyclic structures. The reaction allowed us to synthesize a large range of indole derivatives that may show high biological activity. The designed reaction allows for the synthesis of a variety on C3 alkylated indole derivatives. Mechanistic studies were conducted and allowed us to propose a reasonable mechanism, though that does not completely rule out other possibilities.

3.5. General Information/Experimental Procedures

Unless otherwise noted, all manipulations were carried out under a nitrogen atmosphere using standard Schlenk-line or glovebox techniques. All commercially obtained reagents/solvents were used as received; chemicals were purchased from Alfa Aesar®, Sigma-Aldrich®, Acros ®, TCI America®, Mallinckrodt®, and Oakwood® Products, and were used as received without further purification. Unless stated otherwise, reactions were conducted in oven-dried glassware under nitrogen atmosphere in glove box. Anhydrous DMSO was purchased from Sigma Aldrich and used as received. 1 H NMR, 13C NMR spectra were recorded on Bruker 400 MHz. Both 1H and 13C NMR chemical shifts were reported in parts per million downfield from tetramethylsilane ($\delta = 0$). Data for 1 H NMR are reported as chemical shift (δ ppm) with the corresponding integration values. Coupling constants (J) are reported in hertz (Hz). Standard abbreviations indicating multiplicity were used as follows: s (singlet), b (broad), d (doublet), t (triplet), q (quartet) and m (multiplet). Data for 13C NMR spectra are reported in terms of chemical shift (δ ppm). 19F NMR spectra were obtained at 282.4 MHz, and all chemical shifts

were reported in parts per million, GC-MS analyses were performed on Agilent technologies GC coupled with ESI mass spectrometer.

3.5.1. Preparation of Starting Materials

Indoles **3.17a**, **3.17i-3.17s** were purchased from Oakwood chemicals, Sigma-aldrich, and Alfa Aesar. They were used without any further purification. Compounds **3.17b-3.17h**, and **3.17s-3.17t** were synthesized from the following procedures.

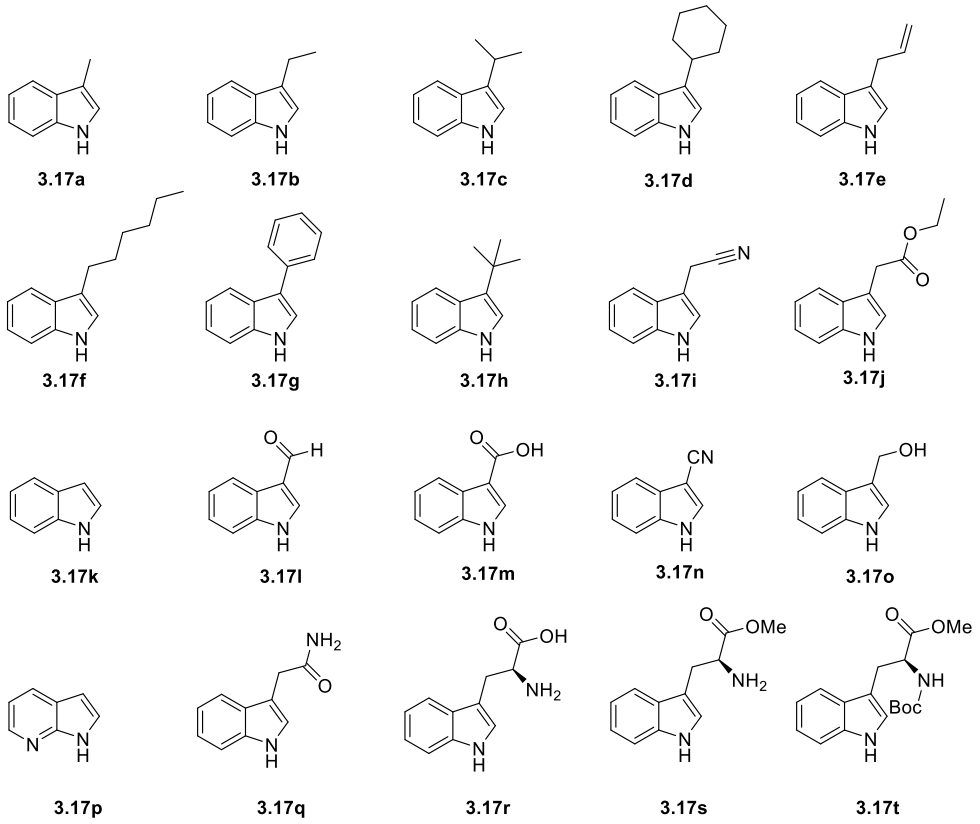

Figure 3.2: Starting material indole substrates.

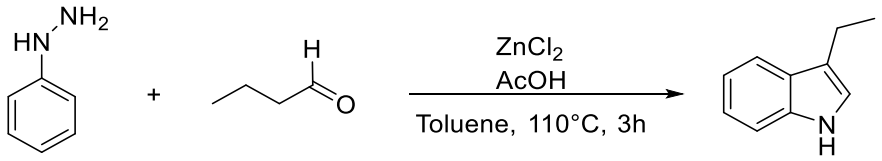

3.17b

Scheme 3.24: Synthesis of starting material **3.17b .**

Indole **3.17b** was synthesized from phenylhydrazine by published procedures[21]. To a solution of phenylhydrazine (540 mg, 5.0 mmol, 1.0 equiv.) and butyraldehyde (0.45 ml, 5.0 mmol, 1.0 equiv.) in toluene (20.0 mL) was added AcOH (0.25 mL, 4.33 mmol, 0.87 equiv). The resulting solution was heated at 110 °C for 30 min. Then, the mixture was cooled to room temperature and concentrated in vacuo. The remaining orange solid was used without further purification. Zinc chloride (341 mg, 2.5 mmol, 0.5 equiv.) was added. The resulting solution was heated at 110 °C for 3 h, then cooled to room temperature. The mixture was washed with brine and extracted with DCM. The organic layers were combined and concentrated in vacuo. The residue was subjected to flash chromatography on silica gel (DCM/n-hexane (1:5) to afford **2b**.

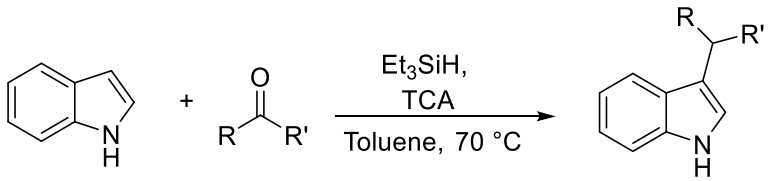

3.17c-d

Scheme 3.25: Synthesis of starting material **3.17c-d.**

In an oven dried flask, triethylsilane (1.63 mL, 10.2 mmol, 2.4 equiv.) and trichloroacetic acid (1.04 g, 6.39 mmol, 1.5 equiv.) were dissolved in toluene (2.1 mL) and the resulting solution was heated to 70 °C[22]. A solution of indole (0.5 g, 4.3 mmol, 1.0 equiv.) and acetone (0.35 mL, 4.8 mmol, 1.1 equiv.) in toluene (2.1 mL) were then added over 1 h. After an additional 20 min at 70 °C the solution was quenched with 10% aqueous solution of sodium

carbonate, the organic layer was separated, dried over anhydrous sodium sulfate, concentrated under reduced pressure, and purified by column chromatography to afford indole **3.17c-d**.

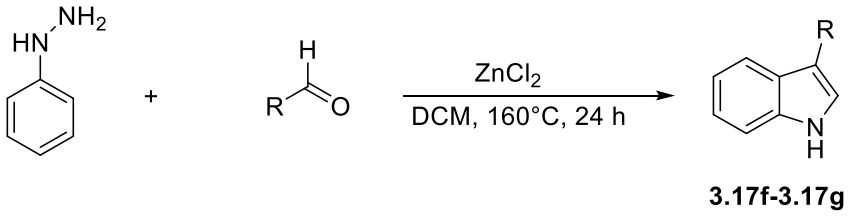

3.17f-3.17g

Scheme 3.26: Synthesis of starting material **3.17f-3.17g**.

To a stirred solution of phenylhydrazine (3.0 g, 28 mmol, 1.0 equiv.) in DCM (20 mL) was added to the corresponding aldehyde (30 mmol, 1.1 equiv.)[23]. After 10 minutes, the solvent was removed under vacuum and the residue was transferred to a three-neck flask equipped with condenser. After adding of p-xylene (25 mL), the mixture was heated to 160 °C and $ZnCl_2$ (8.0 g, 59 mmol. 2.1 equiv.) was added in three portions in 20 minutes. The reaction mixture was stirred at this temperature until the phenylhydrazone was consumed as determined by TLC. After cooling to room temperature, the mixture was extracted with ethyl acetate and washed with brine. The combined organic layer was dried over Na_2SO_4, filtrated, and concentrated under vacuum. The residue was then purified by column chromatography using DCM/Ethyl acetate (1:4) and resulted in indole **3.17f-3.17g**.

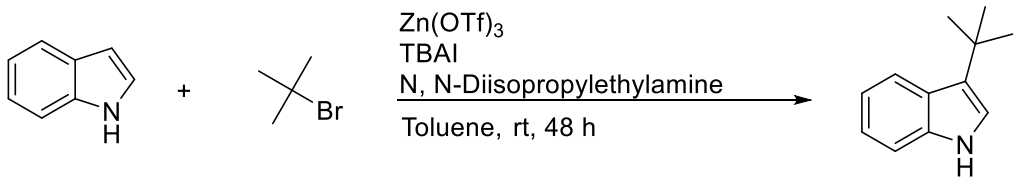

3.17h

Scheme 3.27: Synthesis of starting material **3.17h**.

To a mixture of indole (2.0 g, 17 mmol, 2.0 equiv.), zinc triflate (3.72 g, 10.2 mmol, 1.2 equiv.), and TBAI (3.15 g, 8.53 mmol, 1 equiv.) in anhydrous toluene (52 mL). N.N-

diisopropylethylamine (3.2 mL, 18.8 mmol, 2.2 equiv.) at room temperature under a blanket of nitrogen[24]. After the reaction was stirred 15 minutes at room temperature, t-butyl bromide (2.5 mL, 21.7 mmol) was then added. The reaction solution was stirred at room temperature under nitrogen for 3 hours. Then was extracted with ethyl acetate and washed with brine. The combined organic layers were dried over Na_2SO_4, and the residue was purified via column chromatography (silica, 10% ethyl acetate in hexane) to afford **3.17h**.

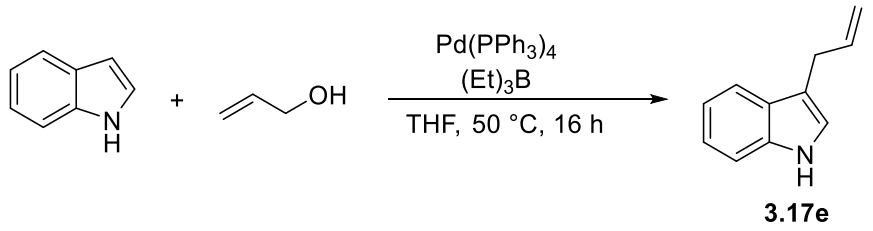

3.17e

Scheme 3.28: Synthesis of starting material **3.17e**.

To a 50 ml two-neck round bottom flask, indole (0.5 g, 4.2 mmol, 1 equiv.) and $Pd(PPh_3)_4$ (0.25 g, 0.21 mmol, .05 equiv.) were added[25]. The round bottom was then evacuated and charged with nitrogen 3x. Then THF (0.2 M), allyl alcohol (0.43 ml, 6.4 mmol, 1.5 equiv.), and BEt_3 (1M) in hexane (0.2 ml, 1.3 mmol, 0.3 equiv.) and the reaction was allowed to stir for 16 h over a nitrogen balloon, The reaction was then quenched with a saturated aq. $NaHCO_3$ solution. It was then extracted with ethyl acetate and washed with brine. Lastly, purified through column chromatography (5% ethyl acetate/hexane) to yield compound **3.17e**.

Starting materials **3.16b-3.16d**, and **3.16g-3.16j** were purchased from commercials sources. Starting materials **3.16e-3.16f** were synthesized from the following procedures.

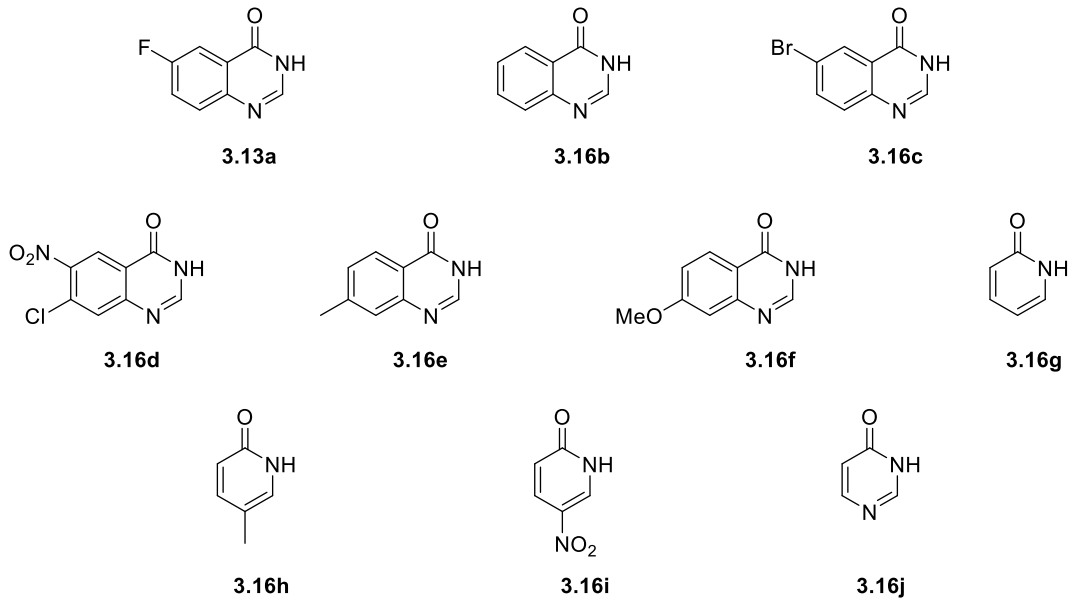

Figure 3.3: N-heterocyclic nucleophile substrates.

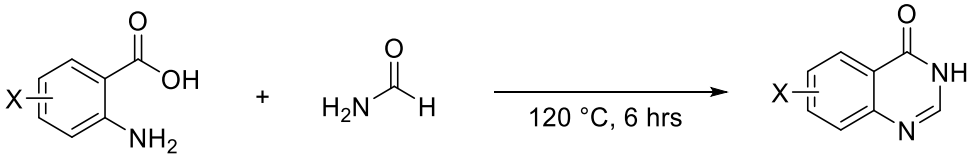

Scheme 3.29: Synthesis of starting material **3.13a, 3.16e-3.16f**.

Benzoic acid (0.5 g ,3.0 mmol, 1 equiv.) was added to an oven dried round bottom flask equipped with a condenser and stir bar[26]. Formamide (0.5 M) was added and the mixture was heated to 120 °C. It was then allowed to go for 6 h. Ice cold water was added to the mixture once it cooled to room temperature. If necessary, 5% $NaHCO_3$ solution was added to the reaction mixture until the pH reached 8. The product proceeded to precipitate from the reaction mixture and was vacuum filtrated to yield product **3.13a, 3.16e-3.16f**. The product was then recrystallized in ethanol to yield a white/tan solid.

3.5.2. General Procedure for Iron Catalyzed C-2 Amidation of Indole

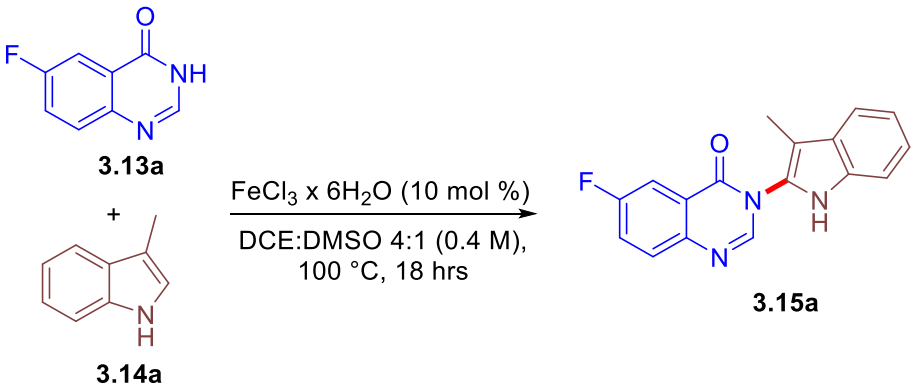

Scheme 3.30: Representative experimental procedure: optimized conditions.

To a 1-dram vial fitted with a teflon cap, under nitrogen atmosphere $FeCl_3$ x 6 H_2O (10 mol %), **3.14a** (0.18 mmol, 1.8 equiv), **3.13a** (0.1 mmol, 1 equiv), and 0.25 ml of DCE:DMSO (4:1) were added simultaneously and stirred at 100 °C for 18 h. The reaction mixture was cooled to room temperature. It was then extracted and washed with ethyl acetate, washed with brine, and dried in sodium sulfate. The reaction mixture was then adsorbed on to silica and purified by column chromatography (Hexane: Ethyl Acetate) to get the product **3.15a** (84%).

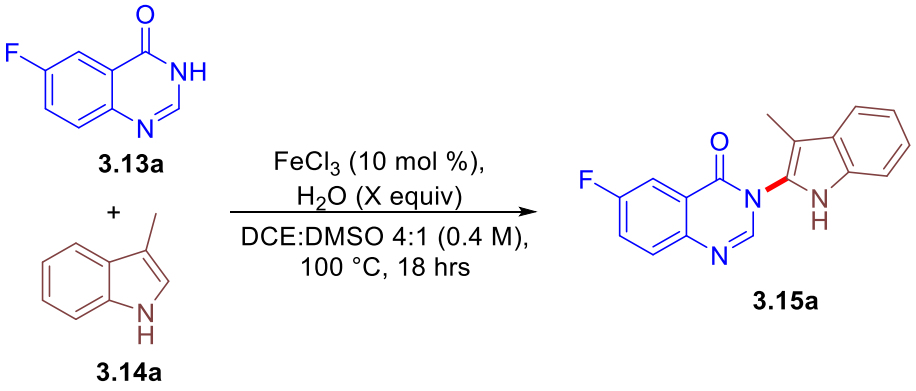

Scheme 3.31: Representative experimental procedure: Water additive study.

To a 1-dram vial fitted with a teflon cap, under nitrogen atmosphere $FeCl_3$ (10 mol %), H_2O (7.6 ul, 2 mmol, 2 equiv.) **3.14a** (0.18 mmol, 1.8 eq.), **3.13a** (0.1 mmol, 1 equiv), and 0.25 ml of DCE:DMSO (4:1) were added simultaneously and stirred at 100 °C for 18 h. The reaction

mixture was cooled to room temperature. It was then extracted and washed with ethyl acetate, washed with brine, and dried in sodium sulfate. The reaction mixture was then adsorbed on to silica and purified by column chromatography (Hexane: Ethyl Acetate) to get the product **3.15a** (81%).

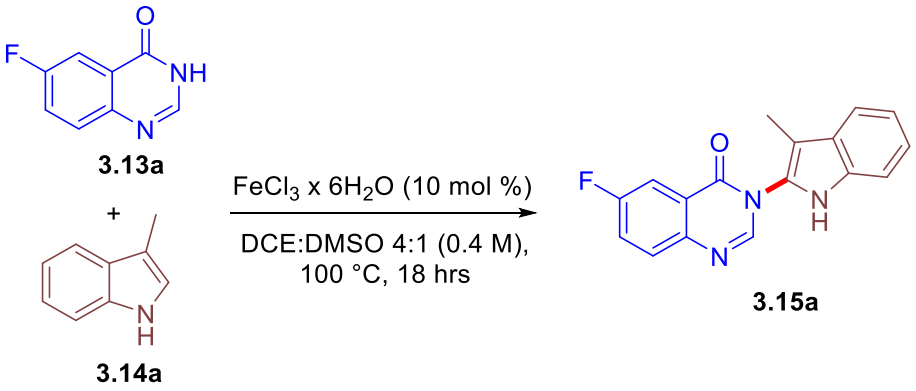

Scheme 3.32: Representative experimental procedure: Scale up study.

To an oven dried 2-neck round bottom flask attached with a condenser, $FeCl_3 \bullet 6H_2O$ (10 mol %), **3.14a** (1.0 mmol, 1.0 equiv), **3.13a** (1.8 mmol, 1.8 equiv) was added. The flask was then evacuated and purged with N_2 3 times. Then (0.4 M) DCE:DMSO 4:1 was added and the reaction was allowed to reflux for 18 h equipped with a nitrogen balloon. Afterwards, the Reaction was quenched with DI water, extracted with ethyl acetate, washed with brine, and allowed to dry under sodium sulfate. Purification was done by column chromatography using 30% ethyl acetate/hexane to yield **3.15a** as light brown/yellow solid.

3.5.3. Analytical Characterization of Purified Compounds

3-(3-Methyl-1H-indol-2-yl)-3H-quinazolin-4-one (3.18a): Prepared by general procedure to yield **3.18a** as a light brown solid (84%); **mp**= 247-251 °C. **^{1}H NMR** (400 MHz, DMSO-d6): 1H NMR (400 MHz, DMSO) δ 11.49 (s, 1H), 8.43 (s, 1H), 8.27 (dd, *J* = 8.0, 1.5 Hz, 1H), 7.95 (ddd, *J* = 8.6, 7.2, 1.6 Hz, 1H), 7.81 (dd, *J* = 8.2, 1.2 Hz, 1H), 7.66 (ddd, *J* = 8.1, 7.2, 1.2 Hz, 1H), 7.61 (dd, *J* = 7.9, 1.0 Hz, 1H), 7.40 (dt, *J* = 8.1, 1.0 Hz, 1H), 7.22 (ddd, *J* = 8.2, 7.0, 1.2 Hz, 1H), 7.11 (ddd, *J* = 8.0, 7.0, 1.0 Hz, 1H), 2.16 (s, 3H). **^{13}C NMR** (101 MHz, DMSO) δ 160.4, 148.1, 148.0, 135.6, 134.3, 128.3, 128.1, 128.0, 127.5, 127.0, 122.9, 122.1, 119.5, 119.5, 111.9, 106.4, 8.1. **HRMS** (ESI-MS) calcd for $C_{17}H_{13}N_3O$ (M + H) 276.1137, found 276.1125.

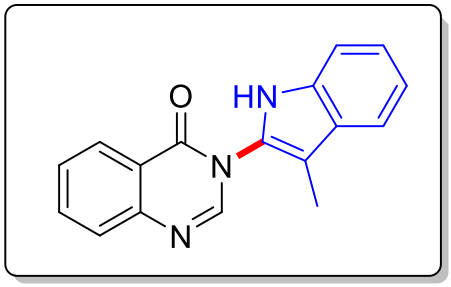

3-(3-*t*-butyl-1H-indol-2-yl)-3H-quinazolin-4-one (3.18h): Prepared by general procedure to yield **3.18h** as a light brown solid (47%); **mp**= 264-269 °C.; **^{1}H NMR** (400 MHz, DMSO) δ 11.37 (s, 1H), 8.50 (s, 1H), 8.26 (dd, *J* = 7.9, 1.6 Hz, 1H), 7.94 (ddd, *J* = 8.5, 7.2, 1.6 Hz, 1H), 7.87 (d, *J* = 8.1 Hz, 1H), 7.81 (d, *J* = 7.7 Hz, 1H), 7.68 – 7.63 (m, 1H), 7.38 (d, *J* = 8.1 Hz, 1H), 7.20 (ddd, *J* = 8.1, 7.0, 1.1 Hz, 1H), 7.09 (ddd, *J* = 8.2, 7.0, 1.2 Hz, 1H), 1.34 (s, 9H).; **^{13}C NMR** (101 MHz, DMSO) δ 161.4, 148.6, 148.1, 135.7, 134.6, 128.4, 128.1, 127.0, 126.0, 125.8, 122.6, 122.3, 121.9, 119.3, 118.9, 112.1, 32.9, 30.9.; **HRMS** (ESI-MS) calcd for $C_{20}H_{19}N_3O$ (M + H) 318.1606, found 318.1599.

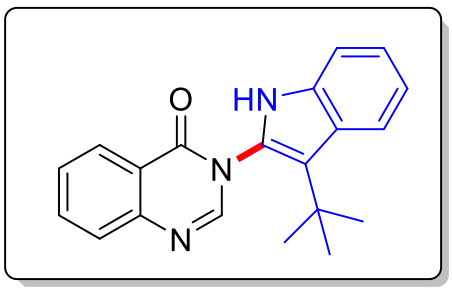

3-(3-Ethyl-1H-indol-2-yl)-3H-quinazolin-4-one (3.18b): Prepared by general procedure to yield **3.18b** as a tan solid (80%); **mp**= 186-196 °C.; **^{1}H NMR** (400 MHz, DMSO) δ 11.47 (s, 1H), 8.42 (s, 1H), 8.27 (dd, *J* = 8.0, 1.5 Hz, 1H), 7.95 (ddd, *J* = 8.5, 7.2, 1.6 Hz, 1H), 7.81 (dd, *J* = 8.2, 1.2 Hz, 1H), 7.66 (ddd, *J* = 8.0, 5.8, 1.3 Hz, 2H), 7.41 (dt, *J* = 8.2, 1.0 Hz, 1H), 7.22 (ddd, *J* = 8.2, 7.1, 1.2 Hz, 1H), 7.10 (ddd, *J* = 8.1, 7.0, 1.1 Hz, 1H), 2.61 (q, *J* = 7.6 Hz, 2H), 1.16 (t, *J* = 7.5 Hz, 3H).; **^{13}C NMR** (101 MHz, DMSO) δ 160.7, 148.0, 135.6, 134.4, 128.4, 128.1, 127.5, 127.0, 126.7, 122.9, 122.1, 119.6, 119.5, 112.8, 111.9, 16.8, 15.1.; **HRMS** (ESI-MS) calcd for $C_{18}H_{15}N_3O$ (M + H) 290.1293, found 290.1288.

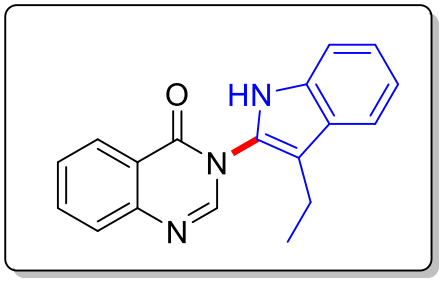

3-(3-Isobutyl-1H-indol-2-yl)-3H-quinazolin-4-one (3.18c): Prepared by general procedure to yield **3.18c** as a tan solid (80%); **mp**= 221-226 °C.; **^{1}H NMR** (400 MHz, DMSO-d6) 1H NMR (400 MHz, DMSO) δ 11.44 (s, 1H), 8.43 (s, 1H), 8.26 (dd, *J* = 8.0, 1.6 Hz, 1H), 7.95 (ddd, *J* = 8.6, 7.2, 1.6 Hz, 1H), 7.81 (dd, *J* = 8.2, 1.2 Hz, 1H), 7.74 (d, *J* = 8.0 Hz, 1H), 7.66 (ddd, *J* = 8.2, 7.3, 1.3 Hz, 1H), 7.46 – 7.36 (m, 1H), 7.21 (ddd, *J* = 8.2, 7.1, 1.2 Hz, 1H), 7.09 (ddd, *J* = 8.1, 7.1, 1.1 Hz, 1H), 2.97 (hept, *J* = 7.2 Hz, 1H), 1.30 (d, *J* = 7.0 Hz, 6H).; **^{13}C NMR** (101 MHz, DMSO) δ 160.9, 148.2, 148.1, 135.7, 134.6, 128.4, 128.1, 127.0, 126.5, 125.6, 122.7, 122.0, 120.5, 119.4, 116.9, 112.1, 25.3, 22.9.; **HRMS** (ESI-MS) calcd for $C_{19}H_{17}N_3O$ (M + H) 304.1450, found 304.1440.

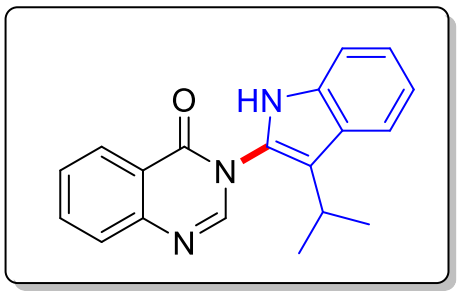

3-(3-Cyclohexyl-1H-indol-2-yl)-3H-quinazolin-4-one (3.18d): Prepared by general procedure to yield **3.18d** as white/tan solid (80%); **mp**= 238-241 °C.; **^{1}H NMR** (400 MHz, DMSO) δ 11.44

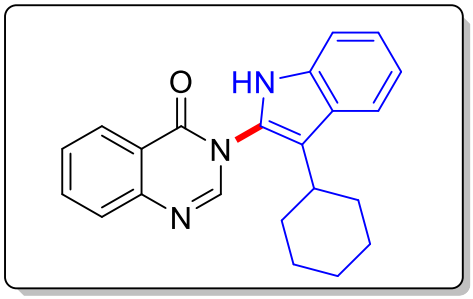

(s, 1H), 8.41 (s, 1H), 8.27 (dd, *J* = 7.9, 1.5 Hz, 1H), 7.95 (ddd, *J* = 8.3, 7.1, 1.5 Hz, 1H), 7.81 (dd, *J* = 8.3, 1.2 Hz, 1H), 7.76 (d, *J* = 8.0 Hz, 1H), 7.66 (ddd, *J* = 8.2, 7.2, 1.2 Hz, 1H), 7.39 (d, *J* = 8.1 Hz, 1H), 7.20 (ddd, *J* = 8.1, 7.1, 1.1 Hz, 1H), 7.08 (ddd, *J* = 8.1, 7.1, 1.1 Hz, 1H), 2.58 (tt, *J* = 11.9, 3.5 Hz, 1H), 1.82 (d, *J* = 12.0 Hz, 2H), 1.76 – 1.60 (m, 5H), 1.35 – 1.14 (m, 3H).; **^{13}C NMR** (101 MHz, DMSO) δ 160.9, 148.2, 148.1, 135.7, 134.5, 128.7, 128.1, 127.1, 126.7, 125.9, 122.7, 122.0, 120.6, 119.3, 116.3, 112.1, 35.6, 32.9, 26.9, 26.1.; **HRMS** (ESI-MS) calcd for $C_{22}H_{21}N_3O$ (M + H) 344.1763, found 344.1754.

3-(3-Allyl-1H-indol-2-yl)-3H-quinazolin-4-one (3.18e): Prepared by general procedure to yield **3.18e** as a brown solid (45%).; **^{1}H NMR** (400 MHz, DMSO) δ 11.60 (s, 1H), 8.38 (s, 1H), 8.26 (dd, *J* = 8.0, 1.6 Hz, 1H), 7.94 (ddd, *J* = 8.5, 7.2, 1.6 Hz, 1H), 7.80 (dd, *J* = 8.2, 1.2 Hz, 1H), 7.70

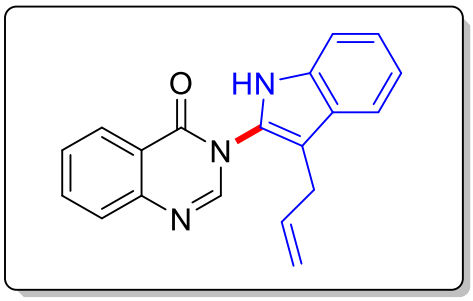

– 7.59 (m, 2H), 7.42 (d, *J* = 8.1 Hz, 1H), 7.22 (ddd, *J* = 8.2, 7.1, 1.2 Hz, 1H), 7.10 (ddd, *J* = 8.0, 7.1, 1.1 Hz, 1H), 5.89 (ddt, *J* = 16.5, 10.0, 6.3 Hz, 1H), 5.02 (dq, *J* = 17.0, 1.8 Hz, 1H), 4.90 (dq, *J* = 9.9, 1.5 Hz, 1H), 3.40 (dt, *J* = 6.4, 1.6 Hz, 2H).; **^{13}C NMR** (101 MHz, DMSO) δ 160.1, 148.0, 147.9, 136.9, 135.6, 134.3, 128.4, 128.3, 128.1, 127.0, 126.8, 122.9, 122.1, 119.7, 119.63, 115.7, 112.0, 108.4, 27.9.; **HRMS** (ESI-MS) calcd for $C_{19}H_{15}N_3O$ (M + H) 302.1293, found 302.1291.

3-(3-n-Hexyl-1H-indol-2-yl)-3H-quinazolin-4-one (3.18f): Prepared by general procedure to yield **3.18f** as a white/tan solid (66%); **mp**= 121-125 °C.; **^{1}H NMR** (400 MHz, DMSO) δ 11.50 (s, 1H), 8.41 (s, 1H), 8.26 (dd, *J* = 8.0, 1.5 Hz, 1H), 7.95 (ddd, *J* = 8.4, 7.2, 1.6 Hz, 1H), 7.81 (dd, *J* = 8.2, 1.1 Hz, 1H), 7.70 – 7.59 (m, 1H), 7.44 – 7.37 (m, 1H), 7.21 (ddd, *J* = 8.2, 7.1, 1.2 Hz, 1H), 7.10 (ddd, *J* = 8.0, 7.1, 1.1 Hz, 1H), 2.59 (t, *J* = 7.5 Hz, 2H), 1.54 (p, *J* = 7.4 Hz, 2H), 1.28 – 1.11 (m, 5H), 1.14 – 1.05 (m, 2H), 0.75 – 0.63 (m, 3H).; **^{13}C NMR** (101 MHz, DMSO) δ 160.7, 148.1, 148.0, 135.6, 134.4, 128.4, 128.1, 127.9, 127.0, 126.9, 122.8, 122.0, 119.6, 119.5, 111.9, 111.3, 31.4, 29.9, 28.7, 23.1, 22.5, 14.3.; **HRMS** (ESI-MS) calcd for $C_{22}H_{23}N_3O$ (M + H) 346.1919, found 346.1908.

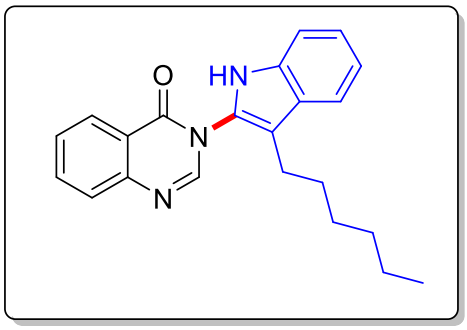

[2-(4-Oxo-4H-quinazolin-3-yl)-1H-indol-3-yl]-acetic acid ethyl ester (3.18*J*): Prepared by general procedure to yield **3.18*J*** as a tan solid (85%); **mp**= 102-107 °C.; **^{1}H NMR** (400 MHz, DMSO) δ 11.77 (s, 1H), 8.38 (s, 1H), 8.26 (dd, *J* = 8.0, 1.5 Hz, 1H), 7.95 (ddd, *J* = 8.6, 7.1, 1.6 Hz, 1H), 7.80 (dd, *J* = 8.2, 1.2 Hz, 1H), 7.74 – 7.61 (m, 2H), 7.44 (dt, *J* = 8.2, 1.0 Hz, 1H), 7.24 (ddd, *J* = 8.2, 7.1, 1.2 Hz, 1H), 7.13 (ddd, *J* = 8.1, 7.1, 1.1 Hz, 1H), 3.95 (q, *J* = 7.1 Hz, 2H), 3.71 (s, 2H), 1.05 (t, *J* = 7.1 Hz, 3H).; **^{13}C NMR** (101 MHz, DMSO) δ 171.1, 160.4, 147.9, 147.7, 135.6, 134.1, 129.2, 128.3, 128.0, 127.0, 126.9, 123.2, 122.2, 119.9, 119.5, 112.1, 104.2, 60.8, 29.6, 14.3.; **HRMS** (ESI-MS) calcd for $C_{20}H_{17}N_3O_3$ (M + H) 341.1348, found 348.1351.

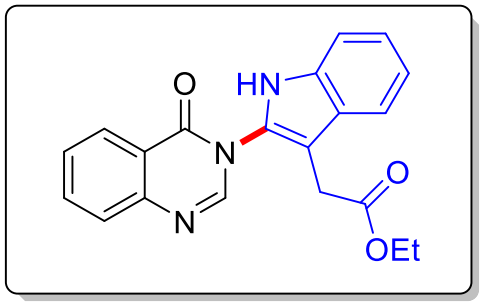

[2-(4-Oxo-4H-quinazolin-3-yl)-1H-indol-3-yl]-acetonitrile (3.18i): Prepared by general procedure to yield **3.18i** as a brown solid (55%); **mp**= 215-220 °C.; **^{1}H NMR** (400 MHz, DMSO) δ 11.93 (s, 1H), 8.44 (s, 1H), 8.27 (dd, *J* = 7.9, 1.5 Hz, 1H), 7.95 (ddd, *J* = 8.5, 7.2, 1.6

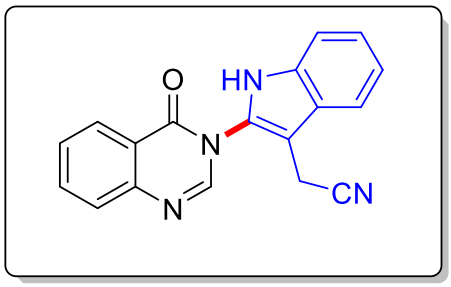

Hz, 1H), 7.81 (dd, *J* = 8.2, 1.2 Hz, 1H), 7.75 (d, *J* = 7.9 Hz, 1H), 7.66 (ddd, *J* = 8.2, 7.2, 1.2 Hz, 1H), 7.51 – 7.45 (m, 1H), 7.30 (ddd, *J* = 8.3, 7.0, 1.2 Hz, 1H), 7.20 (ddd, *J* = 8.1, 7.1, 1.1 Hz, 1H), 4.08 (s, 2H).; **^{13}C NMR** (101 MHz, DMSO) δ 160.5, 147.9, 147.4, 135.6, 134.1, 128.9, 128.3, 128.1, 127.1, 125.9, 123.6, 122.2, 120.4, 119.3, 118.8, 112.3, 100.6, 12.3.; **HRMS** (ESI-MS) calcd for $C_{18}H_{12}N_4O$ (M + H) 301.1089, found 301.1084.

3-(3-Phenyl-1H-indol-2-yl)-3H-quinazolin-4-one (3.18g): Prepared by general procedure to yield **3.18g** as a light brown solid (20%); **mp**= 187-192 °C.; **^{1}H NMR** ^{1}H NMR (400 MHz, DMSO) δ 12.02 (s, 1H), 8.28 (dd, *J* = 7.9, 1.0 Hz, 1H), 8.28 (s, 1H), 7.94 (ddd, *J* = 8.2, 7.2, 1.6

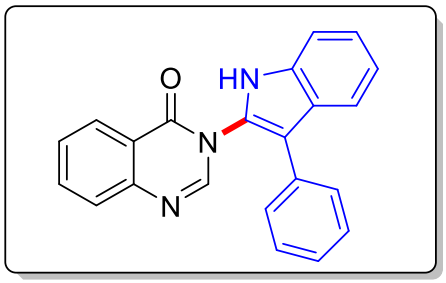

Hz, 1H), 7.75 (t, *J* = 7.7 Hz, 1H), 7.67 (ddd, *J* = 8.3, 7.2, 1.2 Hz, 1H), 7.53 (dt, *J* = 8.2, 1.0 Hz, 1H), 7.39 (d, *J* = 4.3 Hz, 4H), 7.39 – 7.22 (m, 2H), 7.19 (ddd, *J* = 8.1, 7.1, 1.1 Hz, 1H), 3.35 (s, 1H).; **^{13}C NMR** (101 MHz, DMSO) δ 161.2, 148.0, 147.9, 135.9, 134.4, 132.9, 130.1, 129.6, 129.5, 128.7, 128.5, 128.1, 127.8, 127.2, 127.1, 125.8, 123.6, 121.8, 120.8, 120.4, 119.8, 112.4.; **HRMS** (ESI-MS) calcd for $C_{22}H_{15}N_3O$ (M + H) 338.1293, found 338.1283.

3-(3-Methyl-1H-indol-2-yl)-6-flouro-3H-quinazolin-4-one (3.15a): Prepared by general procedure to yield **3.15a** as a brown solid (71%); **mp**= 238-245 °C.; **^{1}H NMR** (400 MHz, DMSO) δ 11.49 (s, 1H), 8.44 (s, 1H), 7.96 (dd, *J* = 8.6, 2.9 Hz, 1H), 7.90 (dd, *J* = 8.9, 5.0 Hz, 1H), 7.83 (td, *J* = 8.6, 2.9 Hz, 1H), 7.61 (d, *J* = 7.9 Hz, 1H), 7.41 (d, *J* = 8.1 Hz, 1H), 7.23 (ddd, *J* = 8.2, 7.0, 1.2 Hz, 1H), 7.11 (td, *J* = 7.5, 7.0, 1.0 Hz, 1H), 2.17 (s, 3H).; **^{13}C NMR** (101 MHz, DMSO) δ 162.4, 159.8, 147.5, 144.9, 134.3, 130.9, 127.8, 127.5, 124.1, 123.8, 123.6, 123.5, 123.0, 119.5, 111.9, 106.5, 8.4.; **^{19}F NMR** (376 MHz, DMSO) δ 111.9.; **HRMS** (ESI-MS) calcd for $C_{17}H_{12}FN_3O$ (M + H) 294.1043, found 294.1034.

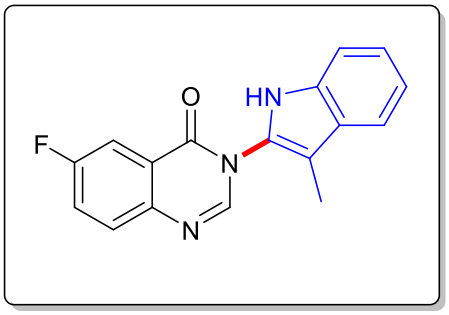

3-(3-Methyl-1H-indol-2-yl)-6-bromo-3H-quinazolin-4-one (3.15b): Prepared by general procedure to yield **3.15b** as a tan solid (77%); **mp**= 259-264 °C.; **^{1}H NMR** (400 MHz, DMSO) δ 11.50 (s, 1H), 8.49 (s, 1H), 8.34 (d, *J* = 2.3 Hz, 1H), 8.10 (dd, *J* = 8.7, 2.3 Hz, 1H), 7.77 (d, *J* = 8.7 Hz, 1H), 7.61 (d, *J* = 7.9 Hz, 1H), 7.41 (d, *J* = 8.1 Hz, 1H), 7.22 (t, *J* = 7.5 Hz, 1H), 7.11 (t, *J* = 7.5 Hz, 1H), 2.16 (s, 3H).; **^{13}C NMR** (101 MHz, DMSO) δ 159.4, 148.6, 147.1, 138.4, 134.3, 130.5, 129.1, 127.7, 127.5, 123.8, 123.0, 120.8, 119.6, 119.5, 111.9, 106.6, 8.1.; **HRMS** (ESI-MS) calcd for $C_{17}H_{12}BrN_3O$ (M + H) 354.0242, found 354.0233.

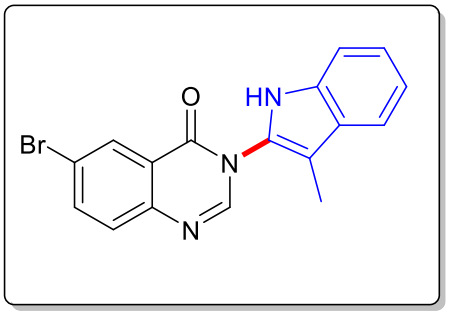

3-(3-Methyl-1H-indol-2-yl)-7-chloro-6-nitro-3H-quinazolin-4-one (3.15c): Prepared by general procedure to yield **3.15c** as a yellow solid (29%); **mp**= 274-278 °C.; **^{1}H NMR** (400

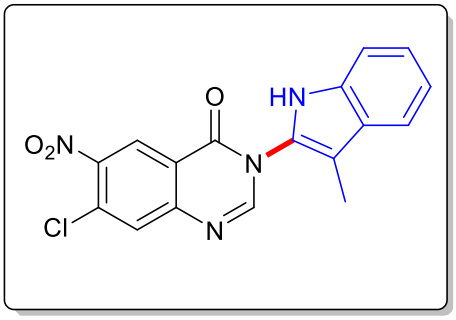

MHz, DMSO) δ 11.47 (s, 1H), 8.84 (s, 1H), 8.68 (s, 1H), 8.21 (s, 1H), 7.62 (d, *J* = 7.9 Hz, 1H), 7.42 (dt, *J* = 8.2, 1.0 Hz, 1H), 7.23 (ddd, *J* = 8.2, 7.0, 1.2 Hz, 1H), 7.12 (ddd, *J* = 8.0, 7.1, 1.1 Hz, 1H), 2.18 (s, 3H).; **^{13}C NMR** (101 MHz, DMSO) δ 159.1, 152.0, 150.8, 146.2, 134.4, 131.6, 130.9, 127.4, 127.1, 125.3, 123.2, 121.5, 119.7, 119.6, 111.9, 106.9, 8.1.; **HRMS** (ESI-MS) calcd for $C_{17}H_{11}ClN_4O_3$ (M + H) 355.0598, found 355.0583.

3-(3-Methyl-1H-indol-2-yl)-7-methyl-3H-quinazolin-4-one (3.15d): Prepared by general procedure to yield **3.15d** as a light brown solid (88%); **mp**= 251-254 °C.; **1H NMR** (400 MHz,

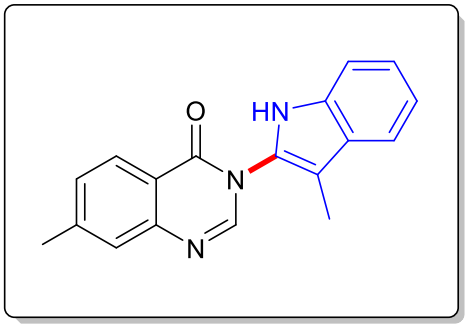

DMSO) δ 11.48 (s, 1H), 8.39 (s, 1H), 8.15 (d, *J* = 8.1 Hz, 1H), 7.65 – 7.57 (m, 2H), 7.52 – 7.45 (m, 1H), 7.39 (dt, *J* = 8.2, 1.0 Hz, 1H), 7.21 (ddd, *J* = 8.2, 7.0, 1.2 Hz, 1H), 7.11 (ddd, *J* = 8.1, 7.0, 1.1 Hz, 1H), 2.53 (s, 3H), 2.15 (s, 3H).; **^{13}C NMR** (101 MHz, DMSO) δ 160.4, 148.1, 148.1, 146.3, 134.3, 129.7, 128.2, 127.7, 127.5, 126.9, 122.9, 119.7, 119.5, 119.5, 111.8, 106.3, 21.8, 8.1.; **HRMS** (ESI-MS) calcd for $C_{18}H_{15}N_3O$ (M + H) 290.1293, found 290.1282.

3-(3-Methyl-1H-indol-2-yl)-7-methoxy-3H-quinazolin-4-one (3.15e): Prepared by general procedure to yield **3.15e** as a brown/orange solid (98%).; **m.p**= 224-231 °C.; **^{1}H NMR** (400

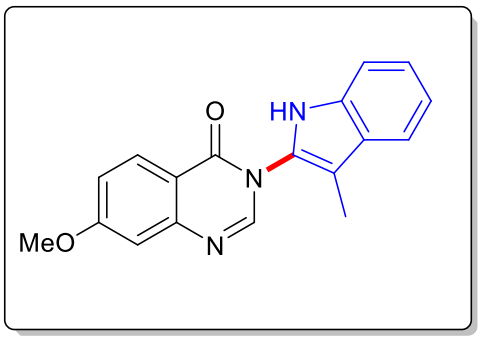

MHz, DMSO) δ 11.48 (s, 1H), 8.40 (s, 1H), 8.16 (d, *J* = 8.7 Hz, 1H), 7.60 (dd, *J* = 7.9, 1.1 Hz, 1H), 7.39 (dt, *J* = 8.1, 1.0 Hz, 1H), 7.27 – 7.17 (m, 3H), 7.10 (ddd, *J* = 8.1, 7.0, 1.1 Hz, 1H), 3.96 (s, 3H), 2.15 (s, 3H).; **^{13}C NMR** (101 MHz, DMSO) δ 165.0, 159.9, 150.3, 148.6, 134.3, 128.7, 128.2, 127.5, 122.9, 119.5, 119.4, 117.5, 115.3, 111.8, 109.4, 106.3, 56.4, 8.1; **HRMS** (ESI-MS) calcd for $C_{18}H_{15}N_3O_2$ (M + H) 306.1242, found 306.1228.

1-(3-Methyl-1H-indol-2-yl)-1H-pyridin-2-one (3.15f): Prepared by general procedure to yield **3.15f** as a brown/orange solid (92%); **mp**= 161-170 °C.; **^{1}H NMR** (400 MHz, DMSO) δ 11.43

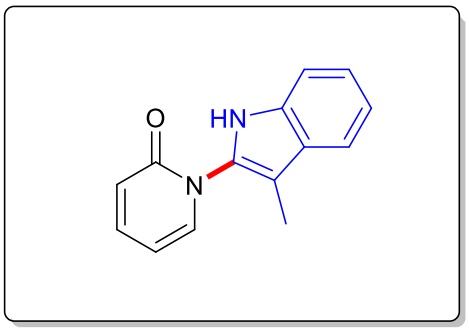

(s, 1H), 7.66 (ddd, *J* = 6.8, 2.1, 0.8 Hz, 1H), 7.62 – 7.52 (m, 2H), 7.34 (dt, *J* = 8.1, 1.0 Hz, 1H), 7.17 (ddd, *J* = 8.2, 7.0, 1.2 Hz, 1H), 7.07 (ddd, *J* = 8.0, 7.0, 1.1 Hz, 1H), 6.55 (ddd, *J* = 9.3, 1.3, 0.8 Hz, 1H), 6.36 (td, *J* = 6.7, 1.3 Hz, 1H), 2.09 (s, 3H).; **^{13}C NMR** (101 MHz, DMSO) δ 161.9, 141.6, 140.3, 134.1, 131.6, 127.5, 122.6, 121.1, 119.3, 119.3, 111.7, 106.1, 104.5, 8.2.; **HRMS** (ESI-MS) calcd for $C_{14}H_{12}N_2O$ (M + H) 225.1028, found 225.1016.

1-(3-Methyl-1H-indol-2-yl)-5-methyl-1H-pyridin-2-one (3.15g): Prepared by general procedure to yield **3.15g** as a tan/yellow solid (90%); **mp**= 156-165 °C.; **^{1}H NMR** (400 MHz, DMSO) δ 11.39 (s, 1H), 7.55 (dd, *J* = 7.9, 1.1 Hz, 1H), 7.50 – 7.42 (m, 2H), 7.33 (dt, *J* = 8.1, 1.0 Hz, 1H), 7.17 (ddd, *J* = 8.2, 7.0, 1.2 Hz, 1H), 7.06 (ddd, *J* = 8.0, 7.1, 1.1 Hz, 1H), 6.50 (d, *J* = 10.1 Hz, 1H), 2.08 (s, 3H), 2.08 (s, 3H).; **^{13}C NMR** (101 MHz, DMSO) δ 161.2, 144.2, 137.0, 134.0, 131.7, 127.6, 122.5, 120.7, 119.3, 119.2, 114.5, 111.6, 104.4, 16.7, 8.2.; **HRMS** (ESI-MS) calcd for $C_{15}H_{14}N_2O$ (M + H) 239.1184, found 239.1177.

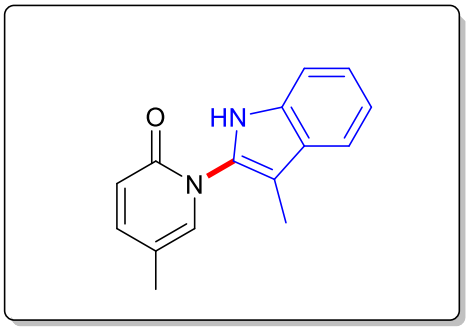

1-(3-Methyl-1H-indol-2-yl)-5-nitro-1H-pyridin-2-one (3.15h): Prepared by general procedure to yield **3.15h** as a yellow solid (46%); **mp**= 215-222 °C.; **^{1}H NMR** (400 MHz, DMSO-d6): ^{1}H NMR (400 MHz, DMSO) δ 11.53 (s, 1H), 9.06 (d, *J* = 3.1 Hz, 1H), 8.29 (dd, *J* = 10.2, 3.2 Hz, 1H), 7.60 (dt, *J* = 7.9, 0.9 Hz, 1H), 7.40 (dt, *J* = 8.2, 1.0 Hz, 1H), 7.22 (ddd, *J* = 8.2, 7.0, 1.2 Hz, 1H), 7.11 (ddd, *J* = 8.0, 7.0, 1.0 Hz, 1H), 6.70 (d, *J* = 10.2 Hz, 1H), 2.14 (s, 3H).; **^{13}C NMR** (101 MHz, DMSO) δ 160.9, 142.6, 134.9, 134.1, 131.1, 129.5, 127.3, 123.2, 119.9, 119.6, 119.6, 111.9, 106.1, 8.2.; **HRMS** (ESI-MS) calcd for $C_{14}H_{11}N_3O_3$ (M + H) 270.0879, found 270.0864.

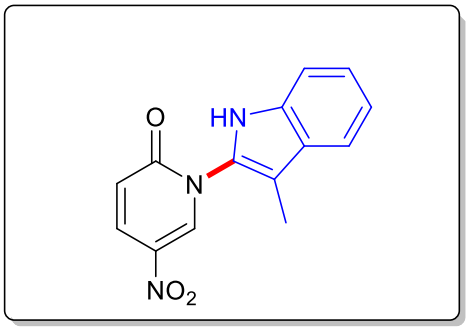

3-(3-methyl-1H-indol-2-yl)-3H-pyrimidin-4-one (3.15i): Prepared by general procedure to yield **3.15i** as a light brown solid (79%); **mp**= 156-160 °C.; **^{1}H NMR** (400 MHz, DMSO) δ

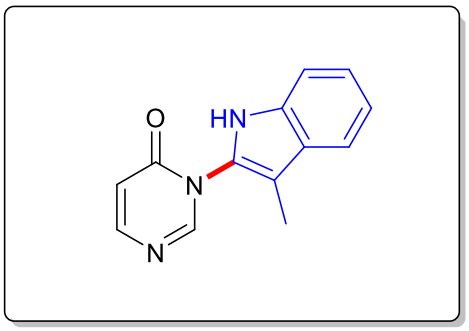

11.50 (s, 1H), 8.54 (t, *J* = 0.8 Hz, 1H), 8.06 (dd, *J* = 6.7, 0.6 Hz, 1H), 7.78 – 7.52 (m, 1H), 7.38 (d, *J* = 8.1 Hz, 1H), 7.21 (dt, 1H), 7.11 (dt, 1H), 6.61 (dd, *J* = 6.8, 1.0 Hz, 1H), 2.12 (s, 3H).; **^{13}C NMR** (101 MHz, DMSO) δ 160.2, 154.3, 153.3, 134.3, 127.7, 127.4, 123.3, 119.6, 119.5, 116.2, 111.9, 106.2, 8.1.; **HRMS** (ESI-MS) calcd for $C_{13}H_{11}N_3O$ (M + H) 226.0980, found 226.0969.

3.6. References

(1) Kumar, S.; Ritika. A. Brief Review of the Biological Potential of Indole Derivatives. *Futur. J. Pharm. Sci.* **2020**, *6* (1), 121. https://doi.org/10.1186/s43094-020-00141-y.

(2) Zhang, M.; Chen, Q.; Yang, G. A Review on Recent Developments of Indole-Containing Antiviral Agents. *Eur. J. Med. Chem.* **2015**, *89* (79), 421–441. https://doi.org/10.1016/j.ejmech.2014.10.065

(3) Thanikachalam, P. V.; Maurya, R. K.; Garg, V.; Monga, V. An Insight into the Medicinal Perspective of Synthetic Analogs of Indole: A Review. *Eur. J. Med. Chem.* **2019**, *180*, 562–612. https://doi.org/10.1016/j.ejmech.2019.07.019.

(4) Lebrasseur, N.; Larrosa, I. Recent Advances in the C2 and C3 Regioselective Direct Arylation of Indoles; Elsevier Inc., 2012; Vol. 105. https://doi.org/10.1016/B978-0-12-396530-1.00004-8.

(5) Bandini, M.; Eichholzer, A. Catalytic Functionalization of Indoles in a New Dimension. **2009**, 48, 9608-9644. https://doi.org/10.1002/anie.200901843.

(6) Wen, J.; Shi, Z. From C4 to C7: Innovative Strategies for Site-Selective Functionalization of Indole C-H Bonds. *Acc. Chem. Res.* **2021**, *54* (7), 1723–1736. https://doi.org/10.1021/acs.accounts.0c00888.

(7) Shi, J.; Zhou, B.; Yang, Y.; Li, Y. Rhodium Catalyzed Regioselective Amidation of Indoles with Sulfonyl Azides via C-H Bond Activation. *Org. Biomol. Chem.* **2012**, *10* (45), 8953–8955. https://doi.org/10.1039/c2ob26767e.

(8) Sun, B.; Yoshino, T.; Matsunaga, S.; Kanai, M. Air-Stable Carbonyl(Pentamethylcyclopentadienyl)Cobalt Diiodide Complex as a Precursor for Cationic (Pentamethylcyclopentadienyl)Cobalt(III) Catalysis: Application for Directed C-2 Selective C-H Amidation of Indoles. *Adv. Synth. Catal.* **2014**, *356* (7), 1491–1495. https://doi.org/10.1002/adsc.201301110.

(9) Sun, B.; Yoshino, T.; Matsunaga, S.; Kanai, M. A Cp∗CoI_2 Dimer as a Precursor for Cationic Co(III)-Catalysis: Application to C-H Phosphoramidation of Indoles. *Chem. Commun.* **2015**, *51* (22), 4659–4661. https://doi.org/10.1039/c4cc10284c.

(10) Kumar, A. S.; Amulya Rao, P. V.; Nagarajan, R. Synthesis of Pyrido[2,3-b]Indoles and Pyrimidoindoles via Pd-Catalyzed Amidation and Cyclization. *Org. Biomol. Chem.* **2012**, *10* (26), 5084–5093. https://doi.org/10.1039/c2ob25371b.

(11) Kumar, A. S.; Nagarajan, R. Synthesis of α-Carbolines via Pd-Catalyzed Amidation and Vilsmeier-Haack Reaction of 3-Acetyl-2-Chloroindoles. *Org. Lett.* **2011**, *13* (6), 1398–1401. https://doi.org/10.1021/ol2000827.

(12) Deka, B.; Deb, M. L.; Baruah, P. K. Recent Advances on the C2-Functionalization of Indole via Umpolung; *Top Curr Chem (Cham)*, **2020**; 378(2), 22. https://doi.org/10.1007/s41061-020-0287-7.

(13) Ghosh, S. K.; Nagarajan, R. NIS-Mediated Regioselective Amidation of Indole with Quinazolinone and Pyrimidone. *RSC Adv.* **2014**, *4* (39), 20136–20144. https://doi.org/10.1039/c4ra02417f.

(14) Luz, E. Q.; Seckler, D.; Araújo, J. S.; Angst, L.; Lima, D. B.; Maluf Rios, E. A.; Ribeiro, R. R.; Rampon, D. S. Fe(III)-Catalyzed Direct C3 Chalcogenylation of Indole: The Effect of Iodide Ions. *Tetrahedron* **2019**, *75* (9), 1258–1266. https://doi.org/10.1016/j.tet.2019.01.037.

(15) Eisenbeis, S. A.; Phillips, J. R.; Rescek, D.; Oyola-Cintron, Y. Synthesis of Azepino[3,4b]Indoles via the Plancher Rearrangement. *Tetrahedron Lett.* **2010**, *51* (33), 4303–4305. https://doi.org/10.1016/j.tetlet.2010.06.029.

(16) Von Dobeneck, H.; Lehnerer, W. Ober Die Oxydation Von Indolderivaten Mit Eisen(III)Chlorid. *Chem. Ber* **1957**, 90, 161–171. https://doi.org/10.1002/cber.19570900203

(17) Tsuji, J; Kexuka, H; Takayanahi, H.; Yamamoto, K. Oxidative Cleavage Reaction of 3-Substituted Indoles Catalyzed by CuCl-Pyridine Complex under Oxygen. *Chem. Soc. Japan* **1980**, *54* (8), 2369–1373. https://doi.org/10.1246/cl.1980.65.

(18) Callan, B.; Manning, A. R. Silver (I) Salts as One-Electron or Two-Electron Oxidants in Their Reactions with $[Fe_2(\eta\text{-}C_5H_5)_2(CO)_4\text{-}n,(CNMe)_n]$Derivatives (n = 0-2).The Effect of Varying the Reaction Solvent. *J. Chem. Soc. Ser. Chem. Commun.* **1983**, 6, 263–264. https://doi.org/10.1039/C39830000263.

(19) Aït-Mohand, S.; Hénin, F.; Muzart, J. Palladium(II)-Mediated Oxidation of Alcohols Using 1,2-Dichloroethane as Pd(0) Reoxidant. *Tetrahedron Lett.* **1995**, *36* (14), 2473–2476. https://doi.org/10.1016/0040-4039(95)00286-3.

(20) Gu, Y.; Jiang, X.; Sun, W.; Bai, S.; Dai, Q.; Wang, X. 1,2-Dichloroethane Deep Oxidation over Bifunctional Ru/CexAly Catalysts. *ACS Omega* **2018**, *3* (8), 8460–8470. https://doi.org/10.1021/acsomega.8b00592.

(21) Zhou, Z.; Li, Y.; Gong, L.; Meggers, E. Enantioselective 2-Alkylation of 3-Substituted Indoles with Dual Chiral Lewis Acid/Hydrogen-Bond-Mediated Catalyst. *Org. Lett.* **2017**, *19* (1), 222–225. https://doi.org/10.1021/acs.orglett.6b03500.

(22) Zhang, Z.; Smal, V.; Retailleau, P.; Voituriez, A.; Frison, G.; Marinetti, A.; Guinchard, X. Tethered Counterion Directed Catalysis: Merging the Chiral Ion-Pairing and Bifunctional Ligand Strategies in Enantioselective Gold (I) Catalysis. *J. Am. Chem. Soc.* **2020**, *142* (8), 3797–3805. https://doi.org/10.1021/jacs.9b11154.

(23) Su, Y.; Hou, Y.; Yin, F.; Xu, Y.; Li, Y.; Zheng, X.; Wang, X. Visible Light-Mediated C-H Diflouromethylation of Electron-Rich Heteroarenes. *Org Lett.* **2014**, 16, 11, 2958–2961. https://doi.org/10.1021/ol501094z

(24) Zhu, X.; Ganesan, A. Regioselective Synthesis of 3-Alkylindoles Mediated by Zinc Triflate. *J. Org. Chem.* **2002**, *67* (8), 2705–2708. https://doi.org/10.1021/jo010996b.

(25) Qi, X.; Chen, P.; Liu, G. Catalytic Oxidative Trifluoromethoxylation of Allylic C−H Bonds Using a Palladium Catalyst. *Angew. Chemie - Int. Ed.* **2017**, *56* (32), 9517–9521. https://doi.org/10.1002/anie.201703841.

(26) Sun, B.; Huang, P.; Yan, Z.; Shi, X.; Tang, X.; Yang, J.; Jin, C. Self-Catalyzed Phototandem Perfluoroalkylation/Cyclization of Unactivated Alkenes: Synthesis of Perfluoroalkyl-Substituted Quinazolinones. *Org. Lett.* **2021**, *23* (3), 1026–1031. https://doi.org/10.1021/acs.orglett.0c04225.